

*OCEAN SCALE AND REGIONAL COMPARISON - ESTUDIOS OCEANICOS Y COMPARACION REGIONAL*

COMPARATIVE CLIMATOLOGY OF SELECTED ENVIRONMENTAL PROCESSES  
IN RELATION TO EASTERN BOUNDARY CURRENT  
PELAGIC FISH REPRODUCTION

by

Richard H. Parrish, Andrew Bakun, David M. Husby and Craig S. Nelson

Pacific Environmental Group  
Southwest Fisheries Center  
National Marine Fisheries Service, NOAA  
P.O. Box 831  
Monterey, California 93942  
USA

In: Sharp, G.D. and J. Csirke (eds), Proceedings of the Expert Consultation to examine Changes in Abundance and Species of Neritic Fish Resources. San Jose, Costa Rica, 18-19 April 1983. FAO Fish Rep. 291 (3): 731-778.

---

### Resumen

Las principales regiones oceánicas del mundo con corrientes marinas en sus confines orientales (i.e., Sistemas de California, Perú, Canarias y Benguela) parecen comportar dinámicas ambientales similares y contienen congregaciones similares de especies de peces pelágicos. En la medida en que especies correspondientes a diferentes sistemas funcionen como análogos, los estudios comparativos interregionales pueden producir información relativa a los efectos del ambiente en el éxito de la reproducción. Lo que de otra forma sería difícil de obtener de un sólo sistema regional.

Los archivos históricos con informes del clima marino proporcionan una fuente de datos en formatos similares sobre la climatología de procesos oceánicos en varias regiones. Estos forman la base para reconocer las diferencias y semejanzas en las diversas áreas de desove de especies correspondientes. La selección natural implica que los hábitos reproductivos en cada caso representan la adaptación a los factores ambientales más cruciales. Por lo tanto los patrones de las relaciones de la reproducción y el ambiente sugieren la existencia de enlaces de causalidad importantes.

Esta forma de deducir los factores ambientales que son cruciales puede dar una base racional para limitar las alternativas en cuanto a las variables que pueden explicar estos procesos. Permitiendo de esta forma el uso más efectivo de las series de datos en la formulación de modelos donde el reclutamiento es dependiente de las condiciones ambientales. Además, el concentrarse en los principales interacciones stock - ambiente puede proveer las bases para utilizar la experiencia que se gana en un sistema para predecir el resultado de acciones en otro sistema.

Normalmente los datos sobre las variables causales primarias (alimento, predación, mortalidad dependiente de la densidad, etc) no están disponibles. Por lo tanto nos concentramos en varios procesos que pueden ser abordados usando datos del mar. Se piensa que estos procesos pueden tener un impacto en los estadios tempranos de la vida de los peces al alterar las variables causales primarias, particularmente el alimento. Estos incluyen: (1) mezcla por turbulencia generada por el viento, que puede dispersar las concentraciones de pequeña escala de las partículas de alimento necesarios para que las larvas se alimenten por primera vez en forma exitosa; (2) transporte mar afuera, que puede arrastrar los huevos y larvas planctónicos fuera de las áreas costeras que le son favorables; (3) afloramientos costeros, que pueden ser favorables si se presentan con un retraso apropiado pero son perjudiciales si coinciden en espacio y tiempo con el desove. La temperatura es una variable causativa primaria por sus efectos directos sobre procesos fisiológicos.

---

Los cuatro principales sistemas de corrientes de los confines orientales del mar tienen mucho en común. La ubicación y estacionalidad del máximo transporte Ekman mar afuera parece estar estrechamente relacionado con el desplazamiento latitudinal y estacional de los sistemas de presión atmosférica y con las relaciones entre estos sistemas y la topografía de los continentes. Sin embargo, como se puede ver de las características ambientales que se presentan, hay también grandes diferencias entre ellas. Por ejemplo, los cuatro sistemas tienen anomalías máximas de bajas temperaturas mar afuera, asociadas con el máximo transporte mar afuera de Ekman de verano. En estas regiones de máximos afloramientos de verano se encuentran stocks de anchoveta y/o sardina con áreas de desove desplazadas hacia el polo y hacia el ecuador. Los sistemas de California y de Benguela tienen, ambos, una sola área con anomalías superficiales de baja temperatura. En el sistema de California esta área está ubicada en el área de máximo afloramiento de verano, mientras que el sistema de Benguela tiene un área de afloramiento máxima de verano en Luderitz y un área de afloramiento máximo de invierno en Cabo Frío. Los sistemas de Perú y las Canarias tienen cada uno dos áreas separadas de anomalías superficiales de baja temperatura. El sistema peruano tiene un área localizada en el área de máximo afloramiento de invierno (San Juan o Chimbote) y una segunda área en la zona de afloramiento frente a la parte central de Chile, que tiene un máximo de verano en Talcahuano. El sistema de Canarias tiene un afloramiento máximo de verano frente a Lisboa y un segundo afloramiento máximo de verano entre Cabo Sim y Cabo Blanc. Durante el invierno la anomalía de aguas frías frente al noroeste de África se desplaza al sur y el máximo del afloramiento se extiende de Cabo Blanc a Cabo Vert.

Los centros de afloramiento (caracterizados por un fuerte transporte mar afuera, intensa mezcla por turbulencia generada por el viento, y reducida estabilidad de la columna de agua) parecen ser evitados como parte de los hábitos de desove. Las áreas de desove de anchovetas y sardinias tienden a estar en las áreas costeras donde el transporte y turbulencia inducidos por el viento son reducidos y la plataforma continental tiende a ser más amplia. Las áreas de desove de las poblaciones más grandes tienden a estar corriente abajo (hacia el ecuador) con respecto a los centros de afloramiento. La población de anchoveta (que ha sido el más grande de todos los stocks actuales de sistemas de corrientes de los confines orientales del mar) desova en un área de fuerte afloramiento. Nuestra hipótesis es que en este caso el ambiente costero particularmente amplio, y la dependencia de la profundidad de la capa de Ekman de la latitud y la estratificación puede servir para reducir el efecto perjudicial del transporte superficial mar afuera de Ekman.

Los patrones para evitar la mezcla por turbulencia y el transporte mar afuera en los hábitos reproductivos sugieren que estos procesos han ejercido un importante control sobre el éxito de la reproducción. Aparentemente estas variables merecen ser consideradas al modelar las variaciones del reclutamiento. En regiones donde las temperaturas características se encuentran dentro de límites fisiológicos, la temperatura no parece ser un factor dominante al determinar el ambiente para el desove.

La capa mínima de oxígeno frente al Perú es muy superficial en comparación con otras regiones. Se sugiere que esto puede conducir a menor competencia entre los stocks de peces pelágicos y los mesopelágicos.

## INTRODUCTION

In this work we have developed climatological fields of oceanographic and meteorological data for the four "classical" eastern boundary current systems (Wooster and Reid, 1963). We attempt, through pattern recognition, to define similarities and differences in the characteristic environmental conditions in the spawning grounds of the recognized stocks of pilchard (Sardina and Sardinops) and anchovy (Engraulis) in these systems. Our approach is similar to Reid's (1967) analysis of the oceanic environs of the genus Engraulis. He included the entire life cycle and described the range of surface temperature and salinity in which Engraulis occurs. We have limited our comparisons to the environments in which the early life history stages occur (i.e., the spawning grounds) and have expanded the list of environmental variables.

A major motivation for international cooperation in fisheries research is the assumption that research methods and/or results derived from studying one population can be transferred to another. For example, the recently proposed "International Recruitment Experiment" (IREX)<sup>2/</sup> is based on the hypothesis that the biological responses to environmental conditions are similar for separate stocks of closely related species. The IREX proposal identifies six variables which are thought to account for most of the biological variability observed in exploited fishes. These variables are temperature, turbulence, transport, food, predation, and population density. Population variations of stocks within a species group, or even in an individual stock, could be caused by any, or all, of the six variables. The hypothesis does not imply that different stocks of a given species group have the same environmental variable as their limiting factor. Rather it implies that the stocks have a similar functional relationship to that environmental variable.

In this work we are addressing a narrow subset within the IREX construct. The species groups considered are anchovies and pilchards, and we are limiting the analyses to comparisons of the environments of their spawning grounds in the four major eastern boundary currents. The regions of interest consist of the California Current off western North America, the Peru Current off western South America, the Canary Current off the Iberian Peninsula and northwestern Africa, and the Benguela Current off southwestern Africa (Fig. 1). Data which could be used to compare the predation, food, and density variables are not available for the spawning grounds of most of the stocks in the California, Peru, Canary, and Benguela Currents. We are therefore basing our comparisons upon several processes which can be indicated by available maritime data. These processes are thought to have important impacts on the early life history of the two species groups by altering the primary causative variables, particularly food. From the point of view of the utility of the study, results based on routinely available data offer the possibility of being followed in real time for management purposes.

Eastern boundary currents are characterized by equatorward surface flow and coastal upwelling. One result of these factors is that the eastern sides of the oceans have a very extensive temperate zone. For example, the 20° and 10°C isotherms at 10 meters occur at lat. 27°N and 60°N in the eastern North Pacific, and in comparison they occur at lat. 40°N and 45°N in the western North Pacific (Barkley, 1968). Another feature of eastern boundary current regions is the tendency for narrow continental shelves. Consequently the fisheries of eastern boundary currents are dominated by a small number of temperate pelagic fishes which can achieve very large populations. The physical environments of the four major eastern boundary currents are quite similar and therefore it is not surprising that their fisheries are dominated by very closely related, geographically isolated stocks or species (Table 1). Pilchards, anchovies, jack mackerel (Trachurus), and hake (Merluccius) achieve the largest populations; mackerel (Scomber japonicus) and bonito (Sarda) also are important in the fisheries of the eastern boundary currents, although they don't attain the population size of the other four species groups.

<sup>2/</sup> Report of Scientific Committee on Ocean Research (SCOR) and Advisory Committee of Experts on Marine Resources Research (ACMRR), Working Group 67 (Oceanography, Marine Ecology and Living Resources) developed in response to the Ocean Sciences in Relation to Living Resources (OSLR) resolution of the Intergovernmental Oceanographic Commission (IOC), 1 July 1982.

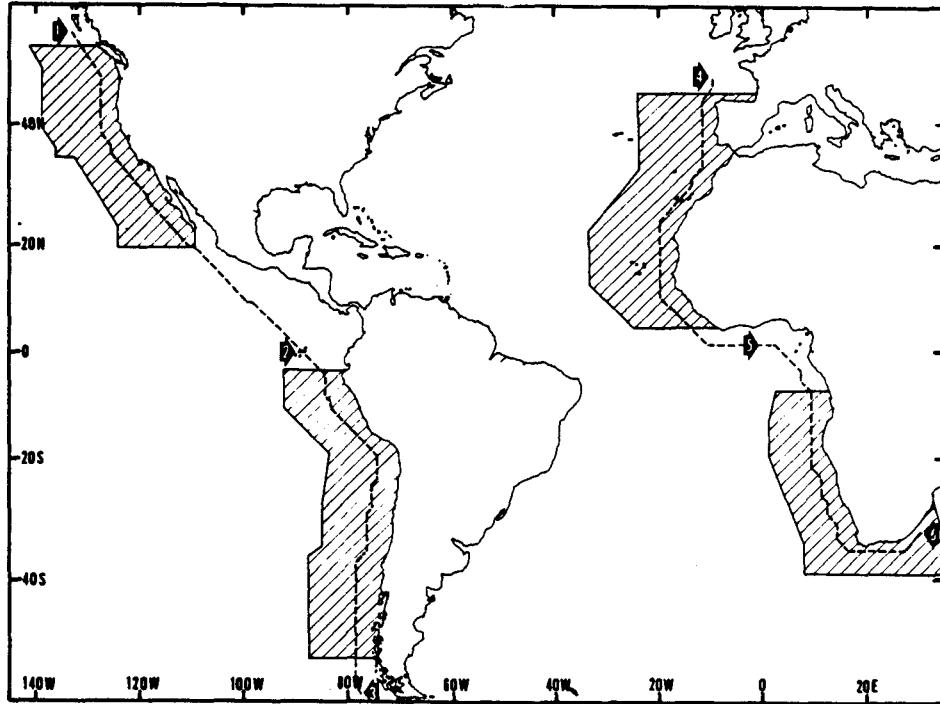


Figure 1. Geographical orientation of various summaries presented in this paper. Appendix maps are assembled from summaries within 1-degree areal segments of the four eastern boundary current regions indicated by diagonal hatching. Along-shore vertical sections (Figs. 3-6) are arranged along the dashed lines near the eastern ocean boundaries.

TABLE 1. Dominant anchovy, pilchard, horse mackerel, hake, mackerel, and bonito in the four major eastern boundary currents (after Bakun and Parrish, 1980).

CALIFORNIA CURRENT	PERU CURRENT	CANARY CURRENT	BENGUELA CURRENT
<i>Engraulis mordax</i>	<i>Engraulis ringens</i>	<i>Engraulis encrasicolus</i>	<i>Engraulis capensis</i>
<i>Sardinops sagax</i>	<i>Sardinops sagax</i>	<i>Sardina pilchardus</i>	<i>Sardinops ocellatus</i>
<i>Trachurus symmetricus</i>	<i>Trachurus symmetricus</i>	<i>Trachurus trachurus</i>	<i>Trachurus trachurus</i>
<i>Merluccius productus</i>	<i>Merluccius gayi</i>	<i>Merluccius merluccius</i>	<i>Merluccius capensis</i>
<i>Scomber japonicus</i>	<i>Scomber japonicus</i>	<i>Scomber japonicus</i>	<i>Scomber japonicus</i>
<i>Sarda chiliensis</i>	<i>Sarda chiliensis</i>	<i>Sarda sarda</i>	<i>Sarda sarda</i>

Fisheries for pilchards and anchovies are notorious for their extreme variability. All four current systems at one time or another have had fisheries dominated by pilchards (Fig. 2). The northern stock in the California Current system (Radovich, 1981) and the Namibian (Troadek, Clark, and Gulland, 1980) and South African (Cram, 1981) stocks in the Benguela Current system have collapsed under heavy exploitation. The Peru Current system (Serra et al., 1979) and the Canary Current system (FAO, 1978) have had recent increases in the size of pilchard stocks, and landings in these regions are presently dominated by pilchards. Conversely, anchovies presently dominate the landings in the Benguela and California Current systems and appear to be abundant, although lightly exploited in the Canary Current system. The collapse of the Peru anchoveta stock under heavy exploitation is well known (Tomczak, 1981).

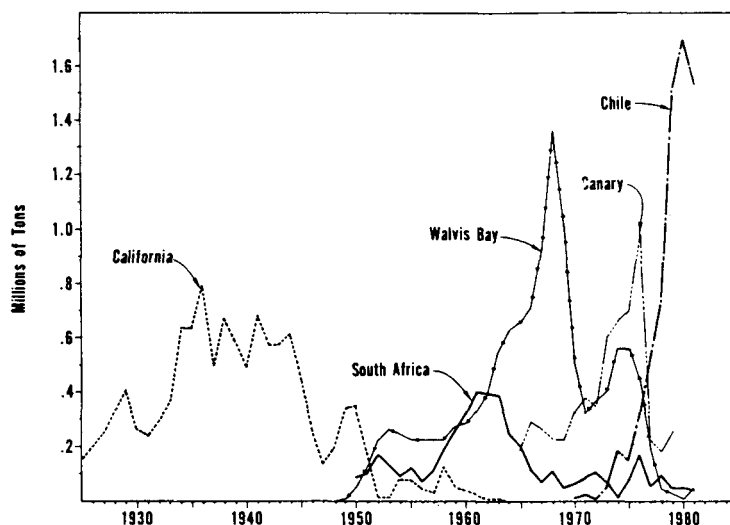


Figure 2. Yearly pilchard (sardine) landings from several eastern boundary current stocks.

The basis for our comparison is, like the IREX proposal, dependent upon the hypothesis that closely related stocks or species have similar early life history requirements. This would suggest that the environments of the various spawning grounds are similar. That is, in the mean they should fall within the tolerance range of the species group. This does not imply that environmental conditions in the spawning grounds are optimal, only that stocks have recently maintained populations by spawning there.

How unrelated may the stocks be before this hypothesis becomes ridiculous? Most fisheries biologists would probably agree<sup>3/</sup> that the present California stock of pilchard (sardine) has the same physiological requirements as the stock had in the 1930's before it collapsed. However, the present remnant of the stock may have a different gene pool than the original. Most fisheries biologists would probably agree<sup>3/</sup> that, within a given species, physiology is nearly identical. Taxonomic distinctions at the species-generic level are quite plastic. The mackerel stocks of the eastern boundary currents are now considered to belong to the same species, Scomber japonicus. Just a few years ago they were considered to be different species and the genus was not Scomber but Pneumatophorus. Each eastern boundary current presently has a different species of Engraulis. These "species" are very similar and it takes considerable expertise to tell them apart. To quote McDowell (1962), "There are grounds for suspicion that this expertise is not possessed by the fish themselves...." We are assuming that in the case of geographically separated stocks of closely related species the differences in the physiological requirements of the early life history stages are negligible.

To provide a basis for our comparisons, historical subsurface oceanographic data and surface marine weather observations are used to examine the large-scale spatial and seasonal patterns of several environmental parameters which appear to have had important effects on the spawning habits of pelagic fishes in eastern boundary current systems. Our comparative studies are primarily focused on the atmosphere-ocean processes related to horizontal and vertical advection, vertical stability, and temperature. Bakun and Parrish (1980) discussed the rationale for selecting the particular suite of oceanic and atmospheric properties described in this study.

Characteristic annual mean distributions of oceanographic data and summer and winter climatologies based on surface marine weather observations are presented in the Appendix as charts of surface geostrophic flow, sea surface temperature and coastal temperature anomaly, surface wind-driven transport, an index of wind-generated turbulent mixing, and total cloud amount. The methods used to compile the climatological data are summarized in the Appendix. The format of placing the charts in an appendix, rather than in the text, was selected to facilitate simultaneous intra- and interregional geographic and seasonal comparisons of the large-scale oceanographic and atmospheric properties.

<sup>3/</sup> A hedge word is always necessary when discussing what fisheries biologists will agree upon.

---

## REGIONAL ASPECTS

The surface flow field in eastern boundary current systems, at least on the time and space scales affecting reproductive success of fish stocks (Parrish, Nelson, and Bakun, 1981) can be considered to be a combination of the surface Ekman drift (i.e., the transport of surface waters under the direct action of the wind) and the underlying geostrophic flow field. Highly smoothed representations of the geostrophic flow patterns in the four regional systems (Appendix Chart 1) show major common features. Near the coast, large-scale flow is generally equatorward. At high latitudes the tendency is poleward. Within several hundred kilometers of the coast, a component of large-scale geostrophic flow toward the coast is a common feature. The far offshore regions are characterized by flow toward the coast in the higher-latitude west wind drifts, weak equatorward flow at mid-latitudes, and flow toward the ocean interiors in tropical regions.

Coastal temperature anomaly patterns (Appendix Charts 5 and 6) indicate a general tendency for cool coastal temperatures relative to those offshore. These patterns show local centers of intense cooling associated with coastal upwelling. There also are relatively warm areas within coastal indentations (responding to seasonal warming) and at the high latitude extremes of the regions (associated with warm advection in the poleward flows).

Surface Ekman transport (Appendix Charts 7 and 8) is generally offshore, but becomes onshore at higher latitudes during the winter seasons. Wooster and Reid (1963) have demonstrated that the major geographical and seasonal features of eastern boundary coastal cooling can be related to corresponding features in offshore Ekman transport. Major capes, marking substantial changes in large-scale coastline trend, tend to be regions of maximum offshore Ekman transport and of associated upwelling and coastal cooling.

## GEOSTROPHIC CURRENT CHARACTERISTICS

The common large-scale features of the eastern boundary currents have been described by Wooster and Reid (1963). The surface flow in these large systems is predominantly in the sense of the prevailing winds, which is anticyclonic about the mid-ocean atmospheric high pressure cells. The weak (typically less than  $50 \text{ cm sec}^{-1}$ ) equatorward geostrophic flow in eastern boundary currents is due to the baroclinicity of a relatively shallow layer, generally confined to the upper 500 m (Wooster and Reid, 1963).

Another common feature of eastern boundary currents is a poleward flowing undercurrent, which is a subsurface current usually centered at 200-300 m near the continental shelf edge. The waters transported poleward by the undercurrents appear to be enhanced by coastal upwelling and may contribute water to the upwelling centers (Smith, 1978). A poleward countercurrent may occur seasonally at the surface during the winter and during periods when the equatorward wind stress weakens.

Coastal countercurrents are often part of semi-permanent eddy circulations, for example, the Southern California Eddy (Sverdrup and Fleming, 1941). A permanent cyclonic circulation over the continental slope and shelf between Cape Frio and south of Lüderitz in southwest Africa has been postulated by Nelson and Hutchings (MS). In the Canary Current region a cyclonic circulation has been observed in the shallow Banc d'Arguin region south of Cap Blanc (Mittelstaedt, 1974) and may be seen in the schematic diagrams of Rebert (1978).

In addition to the narrow coastal currents and the poleward undercurrents, the large-scale surface circulation in eastern boundary current systems is complicated by the effects of bottom topography and coastline orientation. The advent of satellite infrared imagery of the sea surface and intensive hydrographic surveys in the upwelling regions have identified the existence of many eddy-like features or intense frontal zones associated with upwelling sites or downstream of capes and headlands (Bernstein, Breaker, and Whritner, 1977).

---



### California Current System

The major features of the California Current system have been described by Reid, Roden, and Wyllie (1958), Pavlova (1966), and Hickey (1979). The cool, low salinity waters of the west wind drift diverge at about lat.  $45^{\circ}\text{N}$ , one branch flowing north to feed the Alaskan Current and the other branch flowing southeastward to become the California Current. The equatorward flow between lat.  $45^{\circ}\text{N}$  and  $20^{\circ}\text{N}$  and within about 500 km of the west coast encompasses the bulk of the California Current. Maximum equatorward flow occurs approximately 200-400 km from the coast and is strongest in the summer and early fall. A portion of the California Current turns into the coast at about lat.  $30^{\circ}\text{N}$  and is associated with negative wind stress curl in this region (Nelson, 1977). There is a relatively permanent northward flow near the coast between lat.  $30^{\circ}\text{N}$  and Point Conception (lat.  $35^{\circ}\text{N}$ ) which forms the eastern portion of the Southern California Eddy in the Southern California Bight.

The California Undercurrent is a poleward flow of warm, relatively high salinity water at depths of approximately 250-300 m which lies close to the continental slope (Wooster and Jones, 1970). This current is present along the coast from southern Baja California to Vancouver Island (Reed and Halpern, 1976). The northward flow at the surface occurring during the fall and winter along the coast north of Point Conception is commonly called the Davidson Current.

### Peru Current System

The north-northwestward flow north of lat.  $40^{\circ}\text{S}$  has been labelled the Peru or Humboldt Current. Gunther (1936) first recognized two branches of this current: a Peru Coastal Current and a Peru Oceanic Current. The northward flow generally splits into the Coastal and Oceanic Currents at about lat.  $25^{\circ}\text{S}$  (Wyrki, 1965). The annual mean geostrophic flow (Appendix Chart 1) shows this bifurcation at lat.  $25^{\circ}\text{S}$ , long.  $76^{\circ}\text{W}$  and a component of the flow is directed onshore. Both the coastal and oceanic portions of the Peru Current originate in the sub-Antarctic region and transport cold, relatively low salinity water equatorward.

The Peru Countercurrent flows southward at about long.  $80^{\circ}\text{W}$  between the Peru Coastal Current and the Peru Oceanic Current. It is primarily a subsurface current with the strongest flow near 100 m.

The Peru Coastal Current coincides approximately with the upwelling region off Peru and Chile. Coastal bathymetry appears to have considerable influence on the current. Eddies are found wherever the coastal current is deflected strongly from the coast, especially near lat.  $15^{\circ}\text{S}$  (Cañon, 1978). The annual mean surface geostrophic flow is directed onshore north of lat.  $15^{\circ}\text{S}$  and flows strongly onshore in the coastal region between lat.  $10^{\circ}\text{S}$  and  $12^{\circ}\text{S}$ . Wooster and Sievers (1970) noted that the surface drift currents at the coast showed a minimum in equatorward flow between lat.  $12^{\circ}\text{S}$  and  $14^{\circ}\text{S}$  in all seasons, except summer.

During the austral winter the southeast trade winds reach maximum intensity. From April to September the Peru Current appears stronger than in other months and the countercurrent virtually disappears. At this time the two branches of the Peru Current coalesce and the contribution to the South Equatorial Current is the strongest.

The Peru-Chile Undercurrent is a narrow southward flowing countercurrent beneath the Peru Coastal Current. It is found offshore north of lat.  $15^{\circ}\text{S}$ , but south of lat.  $15^{\circ}\text{S}$  it follows close to the coast and can be identified as far as lat.  $48^{\circ}\text{S}$  (Silva and Neshyba, 1979). It is characterized by a low oxygen content.

---

### Canary Current System

The large-scale geostrophic flow in the Canary Current region shows an equatorward component between about lat.  $36^{\circ}\text{N}$  and  $20^{\circ}\text{N}$ . The Canary Current leaves the coast in the vicinity of Cap Blanc (lat.  $21^{\circ}\text{N}$ ), which is also the location of persistent upwelling. Cap Blanc is the site of a semi-permanent frontal zone between the North Atlantic Central Water advected southwest by the Canary Current and a low salinity South Atlantic Central Water mass which flows northward along the coast (Hughes and Barton, 1974).

During periods of weak northerly winds, which occur particularly in summer and autumn between lat.  $10^{\circ}\text{N}$  and  $20^{\circ}\text{N}$ , a coastal northwest-flowing countercurrent may be observed (Mittelstaedt, 1974). This coastal countercurrent gives rise to a cyclonic circulation over the shallow Banc d'Arguin south of Cap Blanc. The coastal countercurrent may be a response to the large discharge of fresh water during the summer from the Gambia and Senegal rivers.

Hughes and Barton (1974) found evidence of a northward flow at a depth of about 250 m extending from Cap Vert to Cabo Bojador. This poleward undercurrent was indicative of a narrow stream of cool, low salinity water flowing parallel to the continental shelf edge.

### Benguela Current System

The major large-scale geostrophic currents off southwest Africa are the equatorward flow between lat.  $35^{\circ}\text{S}$  and about lat.  $20^{\circ}\text{S}$ , which is called the Benguela Current, and the primarily westward flowing Agulhas Current, which flows along the coast of south Africa to approximately long.  $20^{\circ}\text{E}$  where it is deflected to the south and east by the confluence with the west wind drift. A portion of the flow continues toward the northwest around Cape Agulhas and feeds a semi-permanent coastal jet between Cape Agulhas and Cape Columbine (Bang and Andrews, 1974). The principal features of the Benguela Current are described by Hart and Currie (1960).

The Benguela Current consists of the cool upwelled water found within 150 km of the west coast between lat.  $15^{\circ}\text{S}$  and  $34^{\circ}\text{S}$  (Shannon, 1970). In general, it flows northward, roughly following the isobaths between lat.  $34^{\circ}\text{S}$  and  $23^{\circ}\text{S}$ , while north of lat.  $23^{\circ}\text{S}$  it tends to veer away from the coast. Closer inshore a southward moving countercurrent has been occasionally recorded. Hart and Currie (1960) deduced the presence of a southward undercurrent on the continental slope off the Namibian coast from the downwarping of the mid-depth isopycnal surfaces as they approached the continental slope.

The existence of a relatively permanent cyclonic circulation over the continental slope and shelf regions between Cape Frio and a point just south of Lüderitz has been noted by Nelson and Hutchings (MS). The cyclonic circulation is comprised of the northwesterly jet-like flow southwest of Lüderitz where the flow of the Benguela Current accelerates towards the gap in the Walvis Ridge, and a southward return flow near the coast between Cape Frio and Lüderitz. The southward flow near the coast below 30 m has been reported by many investigators. Surface dynamic topography patterns from a series of monthly hydrographic cruises in this area in 1959-61 showed many instances of cyclonic gyres in the region between lat.  $25^{\circ}\text{S}$  and  $20^{\circ}\text{S}$  and southward geostrophic flow north of Lüderitz during spring and summer (Stander, 1964).

---

## DISSOLVED OXYGEN

Minimum oxygen layers are associated with eastern boundary currents. These minimum layers are shallowest and most pronounced in the lower latitudes and more extensive and pronounced in the Pacific than in the Atlantic (Figs. 3, 4). For large-scale comparison of dissolved oxygen and its relationship to the upper mixed layer we developed annual dissolved oxygen and density ( $\sigma_t$ ) sections from data summarized by 1-degree squares. The sections are situated several degrees offshore to allow continuous deep-water sections. This procedure introduces some bias in relation to smaller scale, nearshore features. For example, coastal upwelling or other circulation processes may result in intrusions of low oxygen water into shallower depths on the shelf, which are not indicated by our offshore sections. These intrusions are most likely to occur in the lower latitude areas which are closer to the low oxygen sources. Such intrusions have been reported in the Benguela (Stander and de Decker, 1969) and Peru Currents (Guillén, 1980).

In the California, Canary, and Benguela Currents the minimum oxygen level is altered significantly in the vicinity of the subtropical convergences. The low latitude boundaries of these regions are marked by sharp  $\sigma_t$  gradients associated with the subtropical convergences (Figs. 5, 6). They occur at about lat.  $3^{\circ}\text{S}$  in the Peru Current, lat.  $17^{\circ}\text{S}$  in the Benguela Current, lat.  $22^{\circ}\text{N}$  in the Canary Current, and lat.  $25^{\circ}\text{N}$  in the California Current. The upwelling regions of the eastern boundary currents are also apparent in the density sections; there are few  $\sigma_t$  surfaces intercepting the surface in the upwelling regions. Equatorward of the convergences there is a sharp dissolved oxygen gradient associated with the thermocline and low dissolved oxygen values occur very near the surface. In the Canary and Benguela systems the minimum oxygen layers deepen and disappear in the vicinity of the subtropical convergences (i.e., at about lat.  $20^{\circ}\text{N}$  and  $20^{\circ}\text{S}$ ). In the California Current system the minimum oxygen layer deepens significantly near the subtropical convergence; however, an extensive minimum oxygen layer extends throughout the entire system. Throughout the California Current system low oxygen levels (i.e., less than  $2 \text{ mL L}^{-1}$ ) occur at about 300 m and the oxygen minimum layer occurs at 700-900 m.

The Peru Current is significantly different from the other three currents with respect to dissolved oxygen. The subtropical convergence occurs much closer to the equator and the low oxygen layer expands and shoals in the vicinity of the convergence. The oxygen minimum is at about 300 m throughout the Peru Current system. Off Chimbote, very low dissolved oxygen levels occur just beneath the upper mixed layer. However, at Coquimbo oxygen concentrations of  $2 \text{ mL L}^{-1}$  occur at about 300 m; this is similar to the California Current situation.

Low oxygen concentration could affect reproduction of pelagic fishes through reduction of growth rates of either larvae or adults (Pauly, 1981). It could also increase mortality rates by concentrating the adults or larvae to narrow layers near the surface where they might be more susceptible to predation. However, the "worst" dissolved oxygen conditions occur in the spawning areas of the Peruvian stocks which, at least in the case of *Engraulis*, lie in the most productive region. The other areas most likely to be influenced by low oxygen concentrations are the spawning areas of the Namibian stocks near Palgrave Point in the Benguela Current, and the Chilean stock, which has spawning grounds near Arica. These two areas are the next most productive regions after Peru.

We see two possible explanations for the association of low oxygen concentration and high pelagic fish productivity. Low oxygen concentration is associated with high nutrient concentrations. Low oxygen concentrations near the thermocline might therefore be associated with high primary production; more primary production, hence more fishery production. The other explanation concerns competition. Extensive egg and larval surveys have been made off Peru and California. Ahlstrom (1965) showed that mesopelagic fishes and hake accounted for about 22 percent and 17 percent, respectively, of the total larvae taken off California during the 1955-58 surveys. Both mesopelagic fishes and hake have their greatest abundance below the thermocline (Ahlstrom, 1959). Off Peru mesopelagic fishes and hake comprised only 4.1 and 0.37 percent of the larvae taken during 1966-68 (Santander and de Castillo, 1979). Anchovy larvae comprised 37 percent of the larvae in the California surveys and 92 percent in the Peruvian surveys. The very low oxygen levels just beneath the thermocline off Peru would be expected to severely limit the habitat space for hake and mesopelagic fishes. Habitat space for mesopelagic fishes in the California and Canary systems and most of the Benguela system is extensive and large stocks in these areas would be expected to be in competition with epipelagic fishes for food.

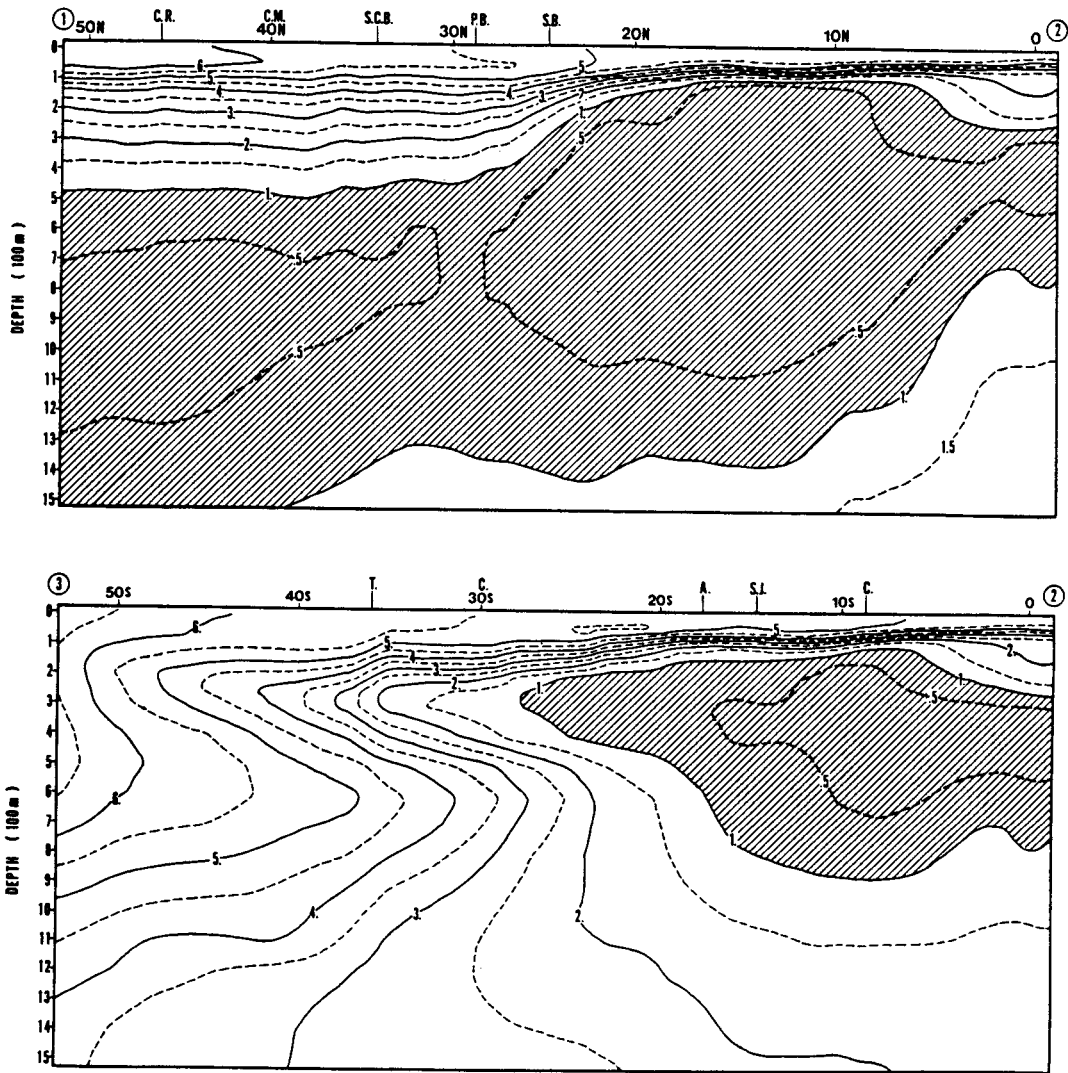


Figure 3. Dissolved oxygen ( $\text{mL L}^{-1}$ ) vs. depth along the eastern boundary of the Pacific Ocean. The orientation of the section is shown in Figure 1. Initials at the top of the diagram indicate the latitudinal positions of locations discussed in detail in Section III of this paper.

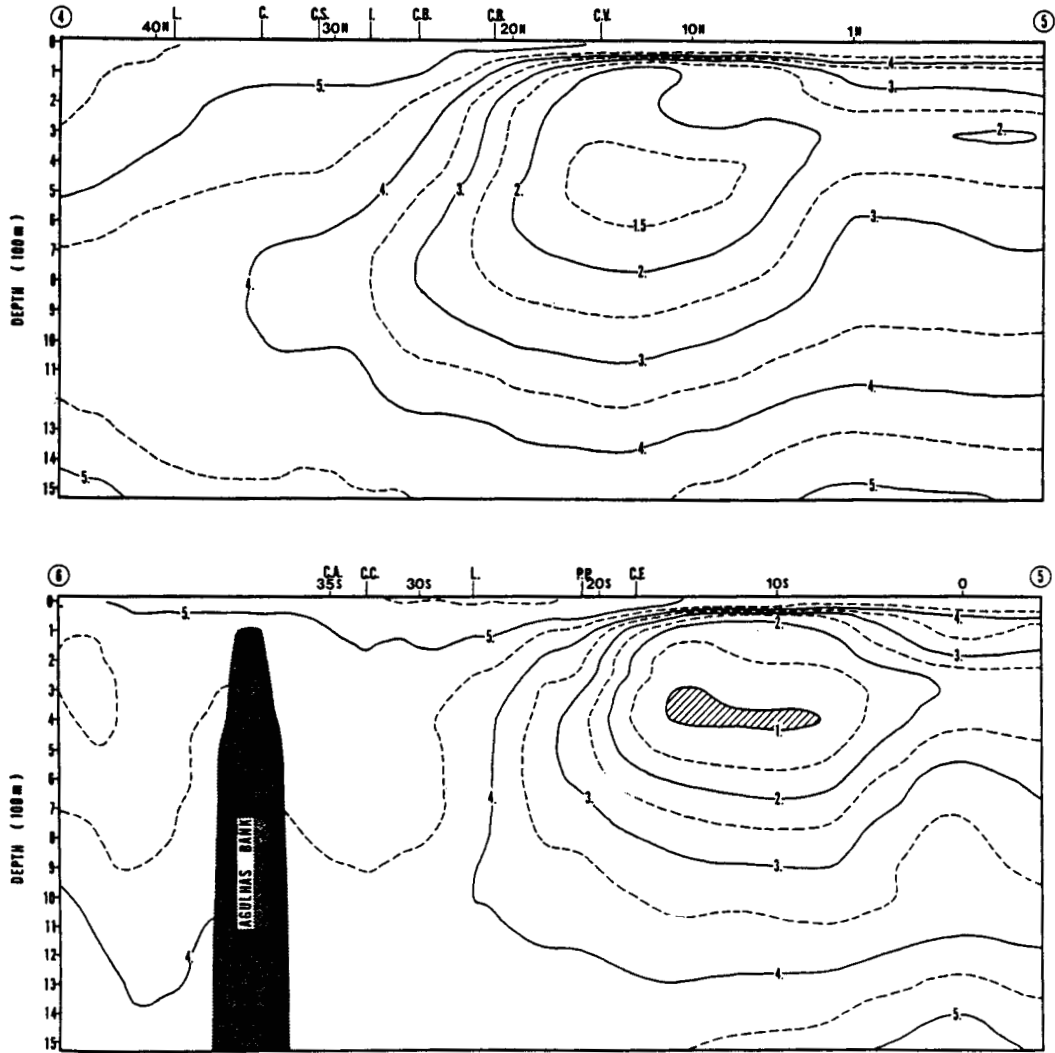


Figure 4. Dissolved oxygen ( $\text{mL L}^{-1}$ ) vs. depth along the eastern boundary of the Atlantic Ocean. The orientation of the section is shown in Figure 1. Initials at the top of the diagram indicate the latitudinal positions of locations discussed in detail in Section III of this paper.

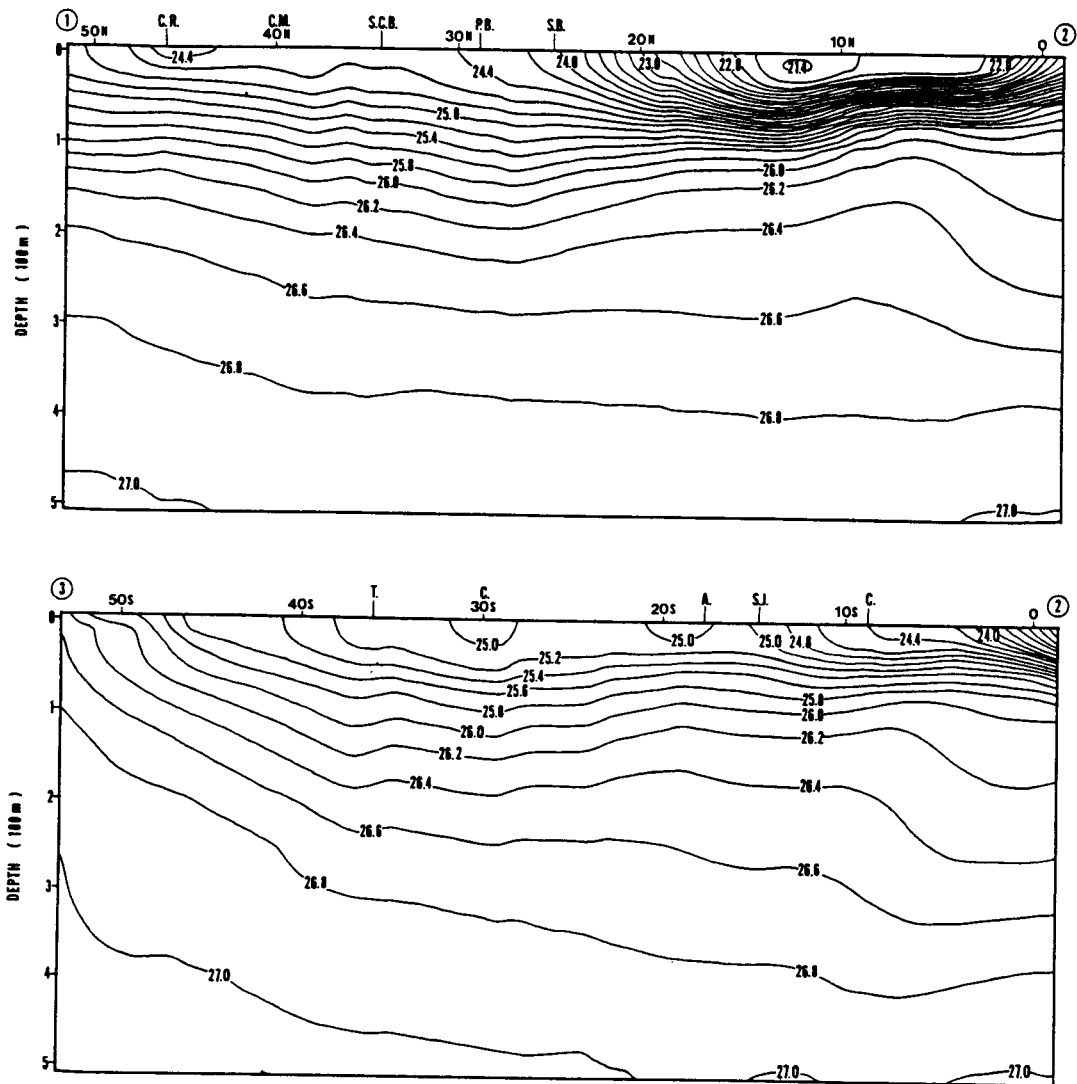


Figure 5. Sea water density ( $\sigma_t$ ) vs. depth along the eastern boundary of the Pacific Ocean. The orientation of the section is shown in Figure 1. Initials at the top of the diagram indicate the latitudinal positions of locations discussed in detail in Section III of this paper.

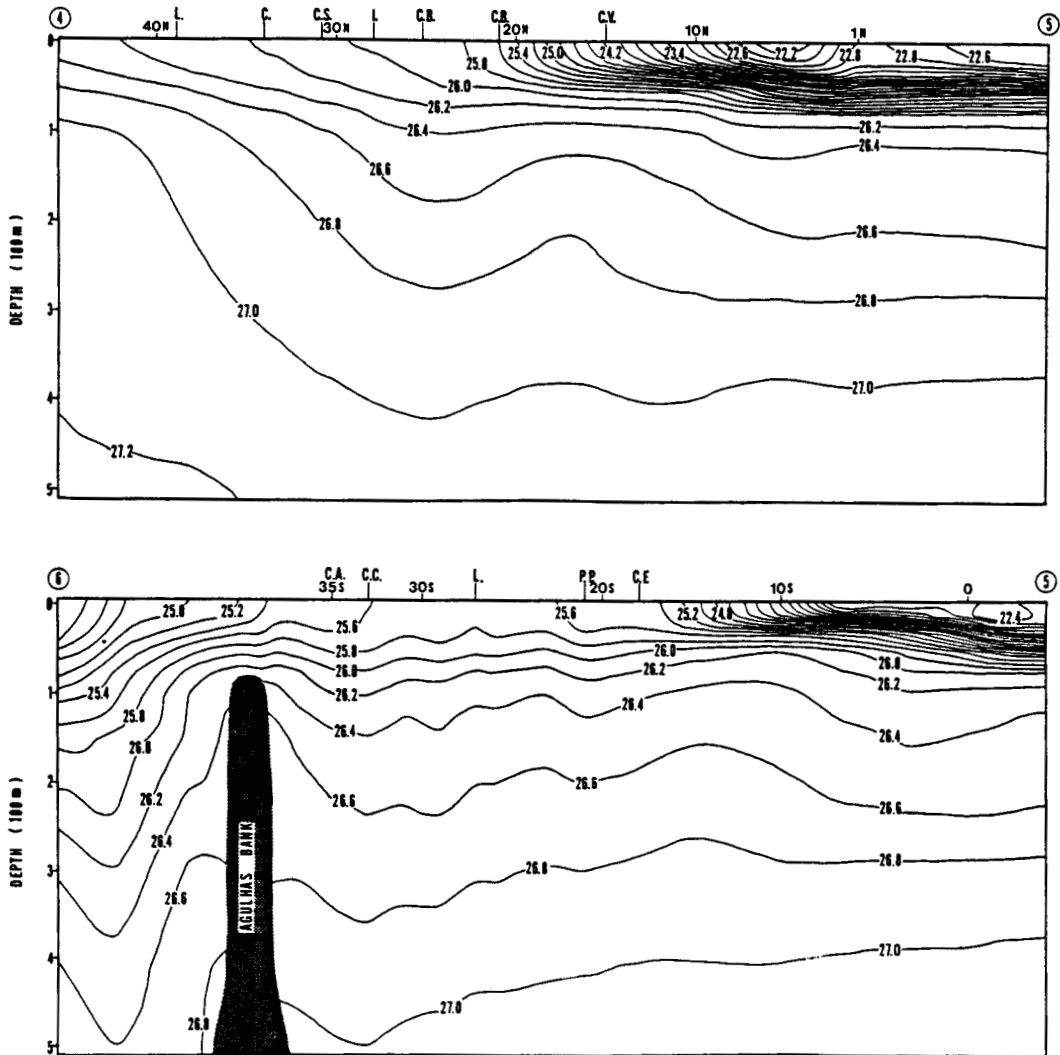


Figure 6. Sea water density ( $\sigma_t$ ) vs. depth along the eastern boundary of the Atlantic Ocean. The orientation of the section is shown in Figure 1. Lines at the top of the diagram indicate the latitudinal positions of locations discussed in detail in Section III of this paper.

### SUBREGIONAL ASPECTS

The charts presented in the appendix are a subset of a considerable volume of material produced and examined in this study. In order to make "cuts" of this material for presentation we have chosen several fixed locations in each eastern boundary region which appear to exemplify the range of environmental characteristics encountered in the near-coastal environments. These locations are labeled in terms of a recognizable feature of coastal geography (i.e., a coastline feature or a coastal city) and appear on the appendix maps and on Figure 7, and are listed in Tables 2 to 4.

Tables 2 and 3 briefly summarize information available on the geography and seasonality of sardine and anchovy spawning in the four eastern boundary current systems. The quality and quantity of information available varies widely among regions and within regions. Thus a fully consistent and complete synthesis is not available to us at this point. Tables 2 and 3 thus should not be considered to be "hard" data, and should not be cited as authority. They are presented as aids to recognition of patterns in the environmental summaries we have assembled (i.e., from the point of view of exploratory data analysis and hypothesis generation rather than of hypothesis testing). Our attempt at preliminary synthesis is intended to generate feedback from workshop participants and others with more specific knowledge of local situations. A discussion of the background and references to Tables 2 and 3 for the California and Peru systems are available in Bakun and Parrish (1982); major references for the Canary system are Bravo de Laguna, Fernandez, and Santana (1976), FAO (1978), and Belvéze and Bravo de Laguna (1980); major references for the Benguela system are King (1977), LeClus (1979), Badenhorst and Boyd (1980), Crawford (1980), and Crawford, Shelton, and Hutchings (1980).

Table 4 lists characteristic sea surface temperature values for 2-month segments of the annual cycle. These values were selected from bimonthly maps of long-term mean summaries which are described in the Appendix and from similar displays of the standard errors of the estimated mean values, in such a way as to characterize the shoreward 50 km of ocean or the locality over which spawning occurs. For example, in the Columbia River Plume, spawning occurs at distances of 100 km or more from the coast and so our presentations attempt to reflect conditions at that location, rather than directly adjacent to the coast.

Figure 7 displays the offshore component of surface Ekman transport plotted against the cube of the wind speed (indicating the rate of addition of turbulent mixing energy to the water column). Table 5 lists values of mixed layer depth obtained from bathythermograph data (Husby and Nelson, 1982). Sparsity of available data restricts this presentation to the California Current locations and the three northern locations in the Peru Current region. Profiles of stability structure for three Benguela locations based on hydrographic data, which lack the vertical resolution provided by bathythermograph traces, are shown in Figure 8. Table 6 contains the widths of the adjacent continental shelves.

---



Table 2. Spawning seasons of Pilchards  
(Relative size of dots is only meaningful at each location)

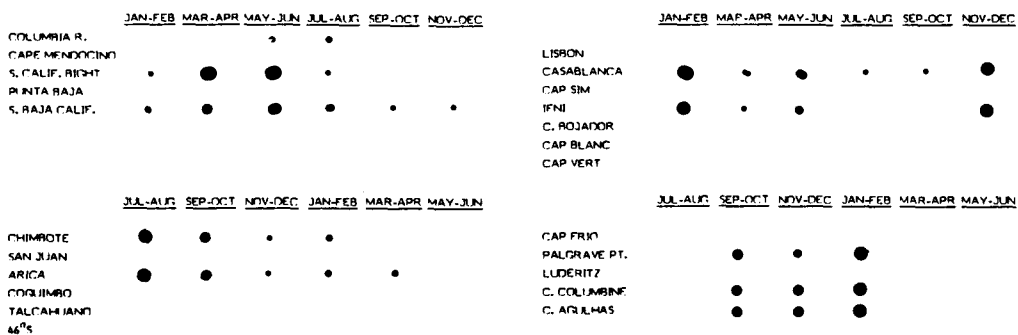


Table 3. Spawning seasons of Anchovies  
(Relative size of dots is only meaningful at each location)

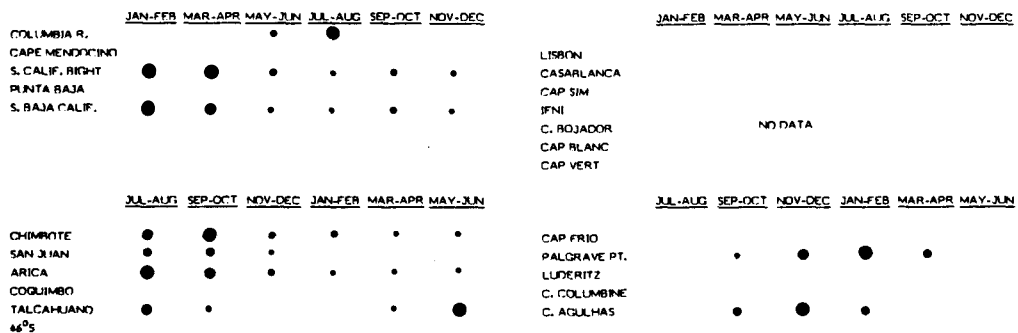


Table 4. Sea Surface Temperature (°C)

Location	JAN-FEB			MAR-APR			MAY-JUN			JUL-AUG			SEP-OCT			NOV-DEC		
COLUMBIA R.	9.2	9.5	12.6	15.1	14.7	11.3												
CAPE MENDOCINO	11.0	10.6	11.1	12.1	12.9	12.1												
S. CALIF. BIGHT	14.0	14.0	16.0	18.0	18.0	15.8												
PUNTA BAJA	16.2	15.5	16.4	19.1	19.5	17.6												
S. BAJA CALIF.	18.9	17.2	17.3	21.8	24.0	21.4												
LISBON	14.0	14.0	16.2	18.0	18.0	15.2												
CASABLANCA	16.4	16.5	18.8	22.3	21.6	18.1												
CAP SIM	16.6	16.9	17.9	18.0	18.7	17.4												
IFNI	17.1	17.6	18.2	19.8	20.0	18.4												
C. ROJADOR	18.1	17.6	19.0	20.5	20.9	20.2												
CAP BLANC	17.7	17.8	18.2	20.6	21.0	19.1												
CAP VERT	19.6	19.5	23.0	27.2	27.8	24.5												
CHIMOTE	17.6	16.9	18.5	21.3	21.1	18.6												
SAN JUAN	15.6	15.1	17.3	19.6	18.1	16.7												
ARICA	16.8	17.6	20.3	22.9	21.8	18.9												
COQUIMBO	13.6	13.5	15.3	17.1	16.5	14.5												
TALCAHUANO	12.0	12.2	14.1	14.9	14.7	13.2												
46°S	8.6	10.8	11.1	13.1	12.7	9.9												
CAP FRIO	14.8	14.9	14.5	18.7	17.3	15.7												
PALGRAVE PT.	14.8	14.2	15.0	18.6	17.6	16.1												
LUDERITZ	13.0	13.0	14.0	15.0	14.0	14.5												
C. COLUMBINE	14.0	14.7	16.0	16.0	15.0	15.0												
C. AGULHAS	15.2	15.8	19.0	20.0	18.4	16.6												

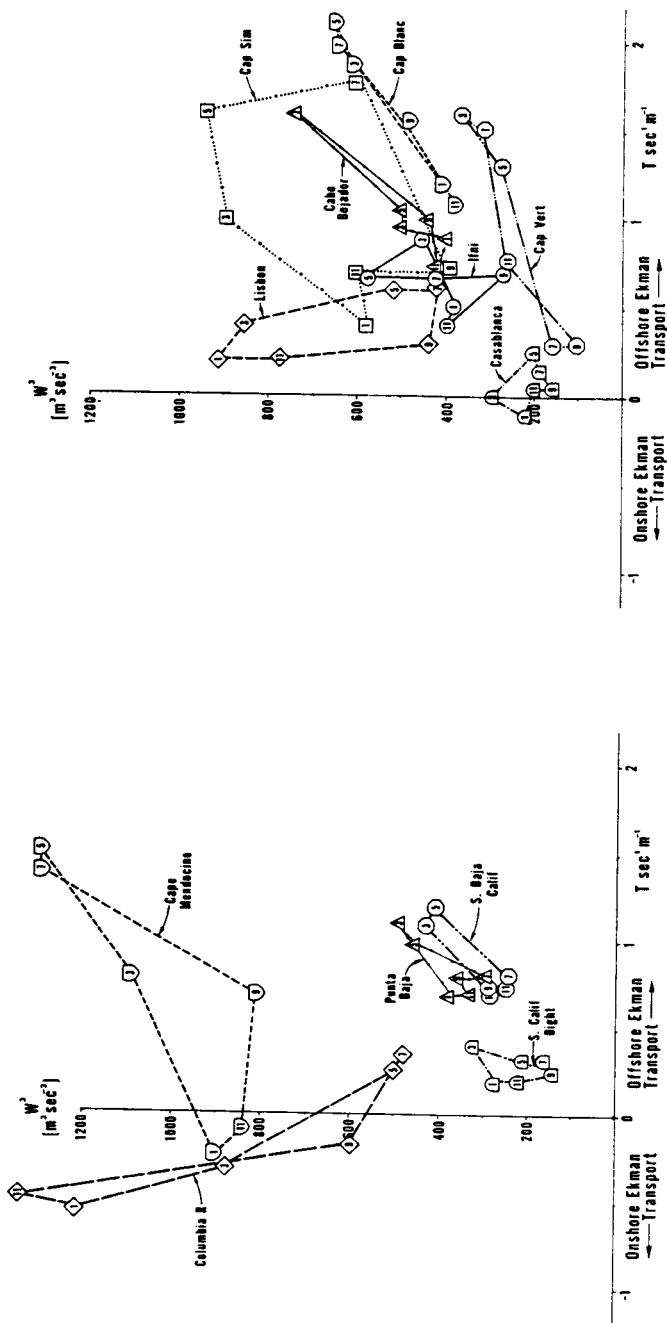


Figure 7. Characteristic seasonal relationships between  $W^3$  (cube of the wind speed) index of turbulent mixing energy production and offshore Ekman transport at various locations in the California, Canary, Peru and Benguela Current systems. Each numbered symbol represents a 2-month climatological sample, with the number corresponding to the first month of the two (e.g., 1 represents Jan.-Feb., 3 represents Mar.-Apr., etc.).

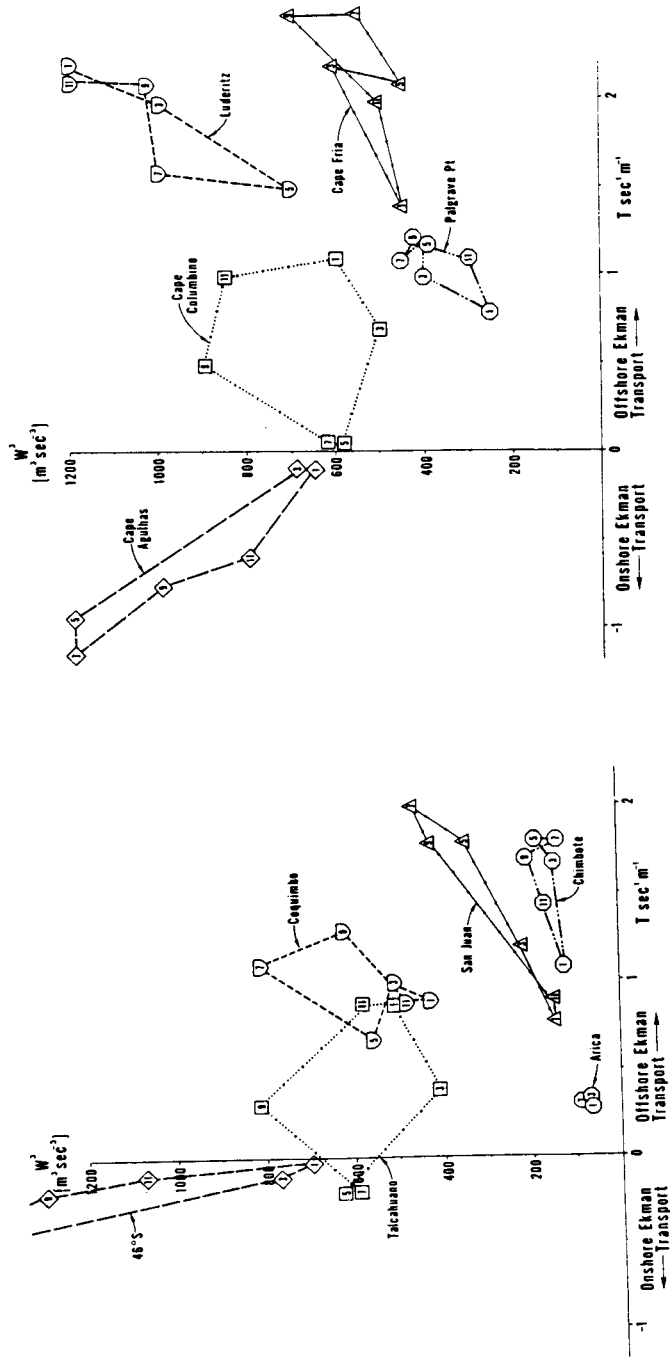


Figure 7. (continued)

Table 5. Mixed layer depths (meters) from historical bathythermograph records.

	<u>JAN-FEB</u>	<u>MAR-APR</u>	<u>MAY-JUN</u>	<u>JUL-AUG</u>	<u>SEP-OCT</u>	<u>NOV-DEC</u>
COLUMBIA R.	103	118	10	10	16	43
CAPE MENDOCINO	-	91	42	28	54	27
S. CALIF. BIGHT	37	25	11	10	14	20
PUNTA BAJA	37	26	18	12	14	26
S. BAJA CALIF.	45	23	18	9	20	34

	<u>JUL-AUG</u>	<u>SEP-OCT</u>	<u>NOV-DEC</u>	<u>JAN-FEB</u>	<u>MAR-APR</u>	<u>MAY-JUN</u>
CHIMBOTE	40	23	12	7	12	29
SAN JUAN	89	87	19	29	20	73
ARICA	14	18	9	5	5	10

Table 6. Approximate width\* of continental shelf (km)

COLUMBIA R.	54	LISBON	43
CAPE MENDOCINO	21	CASABLANCA	56
S. CALIF. BIGHT	168	CAP SIM	38
PUNTA BAJA	29	IFNI	39
S. BAJA CALIF.	71	C. ROJADOR	40
		CAP BLANC	62
		CAP VERT	32
CHIMBOTE	132	CAPE FRIO	32
SAN JUAN	21	PALGRAVE PT.	73
ARICA	53	LUDERITZ	40
COQUIMBO	10	C. COLUMBINE	75
TALCAHUANO	44	C. AGULHAS	128
46°S	93		

\*Distance from coast to 200-m contour (in the case of S. Calif. Bight, distance is to the 200-m contour at the seaward edge of the continental borderland).

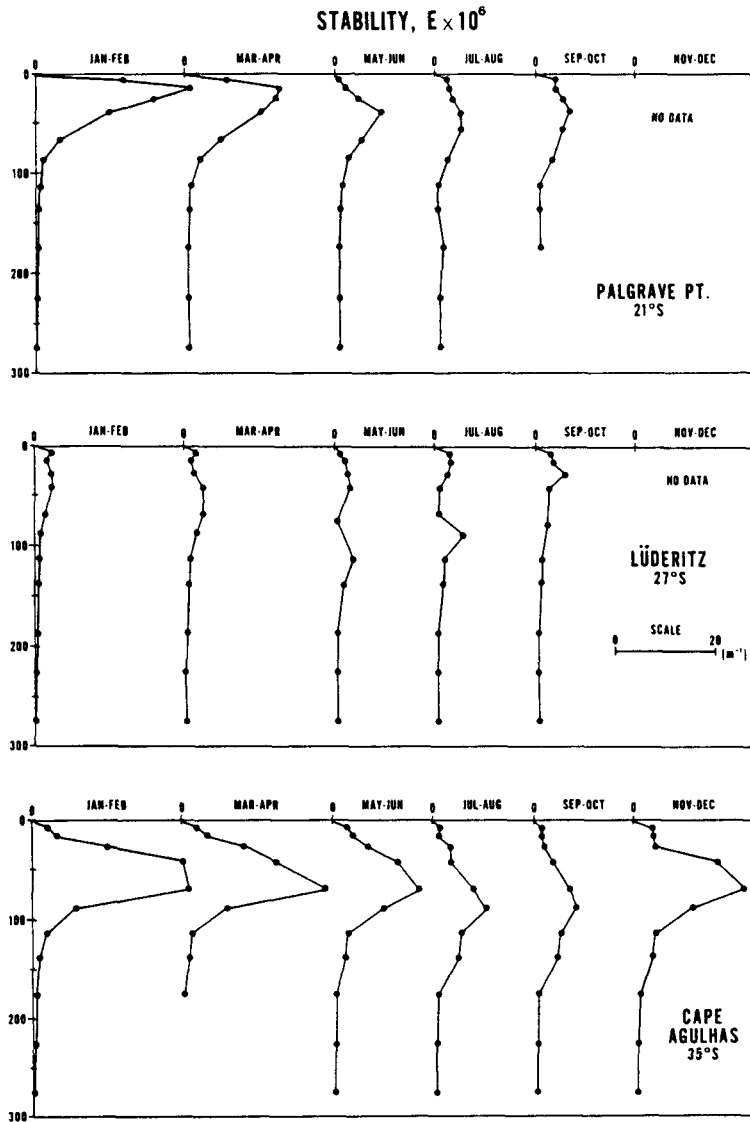


Figure 8. Static stability ( $m^{-1}$ ) vs. depth for 2-month segments (for which there are sufficient hydrographic data to assemble a representative profile) of the seasonal cycles at three locations in the Benguela Current region. Depths are in meters. A scale for magnitude of stability appears to the right on the middle panel.

From these sources and the Appendix maps, the following compressed summary was constructed.

#### CALIFORNIA CURRENT SYSTEM

Columbia River. Anchovy spawning region (only in summer, moderate biomass); moderate continental shelf width; intense wind-generated turbulent mixing, relaxing during summer; stable upper ocean structure during summer due to lens of fresh water at the surface; onshore Ekman transport during winter--weak offshore Ekman transport during summer; little onshore-offshore temperature contrast except very near the coast.

Cape Mendocino. Primary upwelling center; narrow continental shelf; intense offshore Ekman transport, except in winter; intense turbulent mixing throughout the year; intense summer cold coastal temperature anomaly; small biomass of locally spawning fish populations; feeding grounds of adult pelagic fishes spawning elsewhere.

Southern California Bight. The major spawning grounds of pelagic fishes of the California Current; anchovy spawning region (entire year, peaking in winter-spring; large biomass); sardine spawning region (spring, pre-collapse landings 800,000 t); weak offshore Ekman transport; wide continental shelf; moderately weak turbulent mixing; relatively stable upper ocean density structure; warm coastal temperature anomalies extending very near to coast; semi-enclosed inshore gyral circulation pattern.

Punta Baja. Secondary upwelling center; narrow continental shelf; strong offshore Ekman transport, peaking in spring; moderate wind-generated turbulence; lies between two gyral circulations to the north and south and divides areas occupied by separate subpopulations of pelagic fishes. Some spawning occurs (often regarded as contiguous with Southern California Bight spawning populations). Weak negative coastal temperature anomaly.

Southern Baja California. Anchovy spawning region (winter-spring peak, moderate biomass); sardine spawning region (entire year, spring peak--moderate biomass); moderate continental shelf width; strong offshore Ekman transport; weak to moderate turbulent mixing; relatively stable upper ocean density structure; tendency for gyral circulation pattern; warm coastal temperature anomaly.

#### PERU CURRENT SYSTEM

Chimbote. Anchovy spawning region (spring peak, very large pre-collapse biomass); sardine spawning region (winter-spring); wide continental shelf; strong offshore Ekman transport and upwelling; weak wind-generated turbulence; very intense coastal cooling.

San Juan. Upwelling center; intense offshore Ekman transport, particularly in winter; narrow continental shelf; Turbulence level is low in summer, moderate in winter. Less stable stratification than in adjoining areas; very intense coastal cooling; reduced spawning of pelagic fishes relative to neighboring coastal areas (anchovy spawning appears to be intermediate in timing between Chimbote and Arica).

Arica. Anchovy spawning area (winter peak, large pre-collapse biomass); sardine spawning region (winter peak, large biomass); very low turbulence; weak offshore Ekman transport; moderate shelf width; extensive warm coastal temperature anomaly with a narrow band of cooling directly adjacent to the coast; gyral coastal circulation pattern.

Coquimbo. Upwelling center; intense offshore Ekman transport; extremely narrow continental shelf; cold coastal temperature anomalies extending hundreds of kilometers offshore. Turbulence level is moderate in summer, high in winter. No reported pelagic fish spawning.

Talcahuano. Seasonal upwelling (summer); moderate continental shelf width; turbulence level highest in spring; definite spatial minimum in fall and winter turbulence distributions. Anchovy spawning is reported (fall and winter only). Sardine eggs have been found.

46°S. Extreme wind-generated turbulent mixing--much higher than at the same latitude in the California Current region; no reported anchovy or sardine spawning.

---

#### CANARY CURRENT SYSTEM

Lisbon. Moderate upwelling; moderate to high wind-generated turbulence; moderately cool coastal temperature anomaly; moderate continental shelf width.

Casablanca. Sardine spawning region (peak in winter; secondary peak in summer); low turbulence levels (maximum in spring); low Ekman transport; moderate continental shelf width; slightly warm coastal temperature anomaly.

Cap Sim. Upwelling center (strongest offshore Ekman transport in summer); high wind-generated turbulence (minimum in fall); cold coastal temperature anomaly (intense in summer).

Ifni. Sardine spawning region (peak in winter, secondary peak in summer); moderate offshore Ekman transport (strongest in summer); moderate continental shelf width--shelf widens to the immediate south; local minimum in wind generated turbulence.

Cabo Bojador. Strong summer offshore Ekman transport--moderate offshore transport during the remainder of the year; fairly narrow continental shelf; turbulence levels moderate to high (summer maximum); substantial cold coastal temperature anomaly.

Cap Blanc. Upwelling center (intense offshore Ekman transport throughout the year); moderate continental shelf width; strong negative coastal temperature anomaly; moderate turbulent mixing in winter--stronger in summer.

Cap Vert. Highly seasonal upwelling; strong offshore Ekman transport in winter, relaxing greatly in summer; turbulence levels low in late summer and in fall--high in winter and spring; cold coastal temperature anomaly in winter--warm anomaly in summer. Summer and fall temperatures exceed 27°C.

#### BENGUELA CURRENT SYSTEM

Cape Frio. Upwelling center; intense offshore Ekman transport throughout the year, extreme in winter to early spring; strong coastal temperature gradients.

Palgrave Point. Anchovy and sardine spawning grounds (summer); substantial offshore Ekman transport (although much weaker than in the adjacent regions to the north and south--weakest in the summer); fairly wide continental shelf; weak to moderate turbulent mixing--weakest in summer (definite local minimum in the spatial distributions of wind-generated mixing energy production); stable density structure in summer.

Lüderitz. Upwelling center; very intense offshore Ekman transport; moderately narrow continental shelf; intense turbulent mixing--peak intensity in summer; intense cold coastal temperature anomaly throughout the year; low stability in the water column.

Cape Columbine. Sardine spawning grounds (summer--some anchovy spawning); seasonal upwelling; strong offshore Ekman transport in summer, vanishing in winter; moderate continental shelf width; moderate to strong turbulent mixing (spring maximum, fall minimum). A local minimum of turbulent mixing energy production lies within the coastal indentation just to the north of the cape.

Cape Agulhas. Anchovy and sardine spawning grounds (spring-summer); onshore Ekman transport; wide continental shelf; intense turbulent mixing, moderating somewhat in summer; stable ocean structure resulting from a thin lens of warm clear surface water from the Indian Ocean which overlies denser, more productive waters at depth ( 50-75 m).

---

## PATTERN RECOGNITION

Our analyses of the climatological fields and information on spawning grounds suggest the following patterns. Upwelling centers, characterized by strong offshore Ekman transport, intense wind-generated turbulent mixing, reduced water column stability, and narrow continental shelves appear to be areas in which anchovies and sardines do not spawn. Spawning grounds tend to lie in coastal indentations where wind induced transport and turbulence are reduced and continental shelf width tends to be greater. The spawning grounds of the largest populations tend to be located downstream (equatorward) of upwelling centers. Smaller populations (e.g., Columbia River, Talcahuano) are located at the poleward extreme of upwelling regions where the upwelling is highly seasonal, and spawning occurs when various circumstances may reduce the effects of offshore transport and of mixing of the surface layers by the wind.

### Temperature

Sea surface temperature is a better index for establishing cold temperature tolerance than warm temperature tolerance (i.e., it is a good index of the warmest water available but colder water is always available at greater depths). The physiological response of pilchard and anchovy eggs and larvae are best known for the stocks which spawn in the Southern California Bight. Lasker (1964) has shown that pilchard eggs and larvae developed normally between 13° and 21°C; however, larval mortality increased in experiments below 14°C. Incubation time decreased with increasing temperature and early growth was greatest at 16°-17°C. Anchovy eggs and larvae developed normally at 11°C (Lasker, 1964) and early growth was greatest at 21°C in the laboratory (Kramer and Zweifel, 1970).

As long as it does not approach the physiological limits, ambient temperature, at least in so far as it is reflected in sea surface temperature distributions (Table 4 and Appendix Charts 3 and 4), does not appear to exert any obvious control on reproductive habits. For example, seasonal spawning peaks off Southern Baja California and Cape Agulhas correspond to bimonthly temperature values of nearly 19°C, while at Talcahuano peak anchovy spawning occurs in winter at 13°C, even though warmer conditions are available at other seasons. Certainly, temperature conditions exceeding physiological tolerances would preclude occurrence. For example, it is probable that no anchovy spawning would occur in winter off the Columbia River (i.e., at 9°C) even if other conditions were favorable. However, in the regions where the temperatures are within physiological limits, the particular temperature appears not to be a dominant factor in determining spawning habits.

### Turbulence

Spawning rarely occurs in areas of strong turbulent mixing of the upper water column. Spawning grounds are characterized by weak to moderate values of the mean cube of the wind speed, which is an index of the rate of addition of wind-generated turbulent energy to the water column (Husby and Nelson, 1982). Spawning grounds generally lie directly within spatial minima in the  $W^3$  (wind speed cubed) distributions (Appendix Charts 9 and 10). Spawning habitats are characterized by increased stability in the internal density structure of the upper water column (Table 5, Fig. 8) that would resist dispersion of fine-scale food strata by turbulence events related to storms.

Where spawning grounds occur in regions of moderate wind-generated turbulence, other factors influencing stability may be favorable to spawning. For example, off the Columbia River the anchovy population spawns only in the summer (i.e., directly out of phase with other California Current anchovy populations). At this season, the  $W^3$  index falls to moderate values (Fig. 7) and the subsurface stability is enhanced by the thin lens of less dense Columbia River Plume water at the sea surface. At Talcahuano, where turbulence conditions are not greatly lessened during summer, anchovy spawning remains generally in phase with other Peru Current populations; reference to Appendix Charts 9 and 10 will show that turbulent mixing in coastal areas north of Talcahuano is actually less in the winter downwelling season than in the summer upwelling season. Off Cape Agulhas, both anchovy and pilchard populations spawn under conditions characterized by substantial wind-generated mixing. However, this is a situation where particularly strong internal water column stability builds during the summer spawning season (Fig. 8), which may be due to an influx of warm Indian Ocean surface water (Darbyshire, 1966).



### Transport

Areas of intense offshore transport conditions, where reproductive products might be lost from the vicinity of the coast, are characterized by minimum spawning of anchovies and pilchards. In many cases, the effects of transport and turbulence are confounded since strong wind driven offshore transport and strong wind-generated turbulence tend to coincide in eastern boundary upwelling systems. However, adaptations which result in the avoidance of offshore loss of reproductive products appear to be very widespread in fish species successfully inhabiting the California Current region (Parrish et al., 1981), indicating that transport must exact an important control on reproductive success. Note that in two situations where spawning takes place under relatively strong turbulent conditions (i.e., Talcahuano and Cape Agulhas) surface Ekman transport is directed onshore. In addition, Shelton and Hutchings (1982) have shown that a coastal jet between Cape Agulhas and Cape Columbine aids transport of larvae from the spawning grounds to the inshore nursery grounds. At Chimbote an enormous anchovy population has spawned in a situation characterized by strong offshore transport (Fig. 7); this situation is discussed in detail below.

### DISCUSSION

The information presented in this analysis suggests that temperature, transport, and turbulence patterns greatly influence the timing and location of spawning grounds of anchovies and pilchards in eastern boundary currents. Furthermore no single feature has overriding control. It appears that individual stocks have adapted their reproductive strategies to achieve local optimum solutions to these three physical factors. We assume that this also applies to the three factors of the IREX equation which we have not addressed: food, predation, and population density. The question of how good individual optimum solutions are, is probably best judged by the size of the stocks.

The four major eastern boundary currents have a great deal in common. The locations and seasonality of maximum offshore Ekman transport appear to be closely related to the seasonal latitudinal shifts of the atmospheric pressure systems, intensification of the large-scale pressure gradients, and the relationships between these systems and the large-scale topography of the continents. However, as can be seen in the environmental features presented here, there are also large differences among them. For example, all four systems have maximum cold inshore-offshore temperature anomalies associated with summer maxima of offshore Ekman transport. These summer "maximum upwelling regions" have anchovy and/or sardine stocks with spawning grounds poleward and equatorward of them. The California and Benguela systems each have a single area with cold sea surface temperature anomalies. In the California system this area is located in the summer upwelling maximum, whereas the Benguela system's area includes the summer upwelling maximum at Lüderitz and a winter upwelling maximum at Cape Frio. The Peru and Canary systems each have two separate areas of cold sea surface temperature anomalies. The Peru system has an area located at the winter upwelling maximum (San Juan to Chimbote) and a second area in the upwelling region off central Chile which has a summer maximum near Talcahuano. The Canary system has a summer upwelling maximum off Lisbon and a second summer upwelling maximum between Cap Sim and Cap Blanc. During the winter the cold water anomaly off northwest Africa shifts south and the upwelling maximum then extends from Cap Blanc to Cap Vert.

We have noted that spawning of anchovies and pilchards does not occur in the summer upwelling maximum regions, which are characterized by extensive offshore Ekman transport and high wind speed cubed values. Summer mean sea surface temperature values in these upwelling maxima vary from 12°C at Cape Mendocino to 18°C at Cap Sim and Lisbon. Spawning grounds and different stocks generally occur "upstream" and "downstream" of these summer maxima. This suggests that one way to classify the stocks is by their location with respect to upwelling maxima.

Our three classes would be (1) stocks poleward of the summer upwelling maxima, (2) stocks equatorward of the summer upwelling maxima, and (3) stocks equatorward of the winter upwelling maxima. Note that very little is known of the stocks in the lower latitudes of the Canary Current. This classification system also works reasonably well in describing potential fishery yields. Maximum annual yields observed in the higher latitude stocks range from 100,000 to 400,000 tons. Maximum yields in the second group are between 800,000 and 2,000,000 tons. The only stock in the third group, the Peruvian anchoveta, yielded in excess of 10,000,000 tons.

---

The stocks with spawning grounds equatorward of the summer upwelling maxima, with the exception of the stock spawning near Palgrave Point, have a number of features in common. Their spawning grounds (i.e., the Southern California Bight, Arica, Casablanca, and Ifni) are in bights with weak offshore Ekman transport, little inshore-offshore temperature anomaly, and low wind speed cubed values. The anchovy stocks tend to spawn in the late winter - early spring and peak pilchard spawning is either at the same time or just after the anchovy peak. The Palgrave Point spawning grounds occur within an area with a cold inshore-offshore temperature anomaly and spawning in this region occurs in summer when offshore transport and turbulence are at a local minimum. Mean sea surface temperature is in the 14<sup>o</sup>-18<sup>o</sup>C range during the spawning season in all of spawning grounds.

The higher latitude stocks (i.e., those with spawning grounds near the Columbia River, Talcahuano, and Cape Agulhas) are in areas in which turbulence (wind speed cubed) varies seasonally from moderate to high. We have not analyzed the high latitude region of the Canary Current. Ekman transport is onshore during the spawning season in the Talcahuano and Cape Agulhas spawning grounds. The Columbia River region has weak offshore transport during the spawning season and onshore transport during the rest of the year. The Columbia River and Cape Agulhas stocks spawn in the summer when wind speed cubed is at a minimum and spawning occurs in areas where the stability of the water column is increased by intrusions of different water masses (e.g., Columbia River water and Agulhas Current water). The Talcahuano anchoveta stock spawns in the early winter (Jordán, 1980) instead of in the summer when sea surface temperature is at a maximum. We do not know the exact location of this stock's spawning grounds, however, a region of minimum wind speed cubed lies just north of Talcahuano in the early winter.

#### THE PERUVIAN ANOMALY

The anchoveta stock, spawning in the area centered near Chimbote, has been by far the largest stock in the world. We have noted that this area stands out as an anomaly among the major spawning regions in that it is characterized by strong offshore Ekman transport (Fig. 7). Several factors could conceivably be acting to minimize associated offshore loss of reproductive products from this area.

Huyer (1976) has indicated that the offshore extent of coastal upwelling regions may be expanded in regions of wide continental shelves; the continental shelf off Chimbote is much wider than off other upwelling centers (Table 6). Also, the Rossby radius of deformation, which is the intrinsic coastal boundary layer width scale (Moore and Allen, 1973), is inversely dependent on the sine of the latitude. Thus the Rossby radius at Chimbote (lat. 9<sup>o</sup>S) is about twice that at Arica, Palgrave Point, or Cap Blanc, more than 3 times that at Coquimbo, Punta Baja, or Ifni, and about 4 times that at Cape Mendocino or Lisbon.

A more speculative set of considerations concerns the dependence of Ekman layer depth on latitude. The expression for the Ekman depth scale (Ekman, 1905) contains the square root of the sine of the latitude in the denominator. Thus, for comparable vertical eddy viscosities, the Ekman depth at Chimbote would be twice that at Cape Mendocino or Lisbon, for example. For a given magnitude of offshore transport, therefore, the corresponding average offshore velocity of the Ekman layer off Chimbote would be one-half that off Cape Mendocino or Lisbon. Opposing this effect would be the expectation that increasing turbulence input at the higher latitude locations would tend to increase the vertical eddy viscosity which is in the numerator of the Ekman depth expression.

Bakun and Parrish (1982) noted that the peak spawning off Chimbote in winter occurs during the season of strongest offshore transport and hypothesized avoidance of detrimental effects of intermittent El Niño events as a possible reason. An alternate hypothesis concerns Ekman depth which tends to be limited by sharp density discontinuities due to inhibition of vertical eddy viscosity, such that the layer above the discontinuity tends to slide over the denser lower layer which will be relatively unaffected (Neumann and Pierson, 1966, p. 196). The mixed layer depth (Table 5) off Chimbote is much less (7 m) during summer than in winter (40 m). Averaging the corresponding summer (1.1 m<sup>2</sup>sec<sup>-1</sup>) and winter (1.8 m<sup>2</sup>sec<sup>-1</sup>) Ekman transports (Fig. 7) over these depth layers yields average offshore Ekman speeds of approximately 0.04 m sec<sup>-1</sup> (3.5 km d<sup>-1</sup>) in winter and 0.16 m sec<sup>-1</sup> (14.0 km d<sup>-1</sup>) in summer. Planktonic reproductive products within the mixed layer would thereby be dispersed offshore four times as rapidly during summer than during the winter spawning peak.

---

## IMPLICATIONS FOR POPULATION MODELING

Fishery time series are generally quite short and often contain only one to several realizations of major shifts in trend (e.g., Fig. 2). The result is that there are often insufficient degrees of freedom for purely empirical approaches to be effective in defining relationships with multiple environmental factors. Thus it is important to incorporate as much accessory information as can be gleaned independently from the actual time series data. Accessory information can come from process-oriented experiments or from various deductive approaches such as the one we have presented in this paper.

The most straightforward way to incorporate this sort of information is in the choice and formulation of the explanatory variables. By choosing a very limited set of variables which addresses only those processes which appear to be the most crucial and by formulating these variables specifically according to the manner in which they appear to affect the populations, the degrees of freedom available in the time series can be expended with the greatest likelihood of generating beneficial information (Bakun and Parrish, 1980).

In this study we have compared seasonality and geography of reproduction with corresponding features in the environment. Since natural selection implies adaptation of reproductive strategies to the most crucial processes affecting reproductive success, patterns of correspondence may illuminate the environmental linkages.

We have noted that spawning tends not to occur in regions characterized by wind conditions which would generate intense turbulent mixing of the upper water column. This would tend to support Lasker's (1978) mechanism for larval mortality caused by wind-generated turbulent dispersion of fine-scale strata of food particles appropriate for first-feeding. Some degree of information on surface wind conditions is generally available. In view of the hypothesized mechanism, the average turbulence generation over monthly or longer intervals is probably not the ideal way to formulate this variable. Rather, the frequency and duration of periods where wind speeds do not exceed a critical threshold, above which it would breakdown the underlying water column stability, may be more pertinent considerations (Husby and Nelson, 1982). No specifics of such a formulation have been proposed.

Another pattern in reproductive strategies is the absence of spawning in regions characterized by strong offshore transport whereby reproductive products are lost. This mechanism tends to be confounded with the turbulence mechanism in the situations we are examining. For example, in upwelling centers, strong offshore transport coincides with intense turbulence generation. However, we have noted indications that the transport mechanism is acting (i.e., in certain situations where characteristic transport is not directed strongly offshore, spawning occurs under conditions which appear to be typified by substantial wind-generated turbulence). We have also speculated that the seasonality of spawning at Chimbo is tuned so as to minimize offshore dispersion of reproductive products, rather than to minimize turbulent mixing.

As is the case for the turbulence indices, estimates of offshore Ekman transport (e.g., Bakun, 1973) can also be generated from wind information. However, the two mechanisms imply distinctly different time scales. The turbulence mechanism acts to cause larval starvation on a time scale of a few days; it is non-linear in that water once mixed is not unmixed by reversing the action of the wind. The transport mechanism acts on much longer time scales and may indirectly cause mortality of late larvae and juveniles by displacing them from the favorable coastal environments. Transport is linearly additive; a period of offshore transport could be counteracted by a later period of onshore transport.

No pattern has emerged to indicate that reproductive strategies are strongly influenced by an optimum temperature. Obviously, the physiological temperature limits of the organisms provide barriers to reproduction in extreme cases. This analysis suggests that the effective way to incorporate temperature data in an empirical recruitment model may be simply as an indicator variable which has a value of "one" for a range of temperatures within which spawning can occur and "zero" beyond that range. An additional temperature effect, which may become significant once the variance due to the indicator variable is accounted for, may occur due to increases in physiological rates, etc., by increases in temperature within the generally favorable range.

---

## APPENDIX

### OCEANOGRAPHIC DATA

To assemble characteristic distributions of the large-scale oceanographic features in the four boundary current regions, we used existing global summaries of subsurface data. Objectively analyzed fields of annual mean temperature, salinity, and oxygen at standard depths were provided by Sydney Levitus of the National Oceanic and Atmospheric Administration's (NOAA) Geophysical Fluid Dynamics Laboratory (GFDL). Data sources and analysis methods and selected horizontal distributions and vertical sections are described in detail by Levitus and Oort (1977) and Levitus (1982).

The annual mean geostrophic flow at the surface was constructed from the analyzed fields of temperature and salinity defined on a grid of 1-degree latitude by 1-degree longitude in each of the eastern boundary current regions. Dynamic topographies relative to the 1000 db level (approximately 1000 m) were computed following LaFond (1951). The computation points for surface velocity are offset from the values of dynamic height by a half-degree in both directions (i.e., calculated velocities are centered on the whole degree of latitude and longitude). Therefore, a velocity vector for each 1-degree square was calculated from the gradients defined by dynamic height values at the corners of each square. To clarify the presentations shown in Chart 1, vector symbols are only plotted for alternate 1-degree squares in both latitude and longitude coordinates. Contours of dynamic height (in dynamic meters, with a contour interval of 0.04 dyn m) are superimposed on the vector fields as an aid to interpreting the flow direction and strength (i.e., the surface geostrophic flow is parallel to contours of dynamic height and the current speed is inversely proportional to the contour spacing and to the sine of the latitude). Directions are defined such that higher values of dynamic height lie to the right (left) of the current in the northern (southern) hemisphere when facing in the direction of flow.

The analyzed fields from which these velocity calculations have been made were designed for global, rather than regional studies of ocean circulation. Well recognized seasonal variations in surface current features are not depicted in the annual mean distributions. For example, where speeds represented in Chart 1 vary from 2 to 10 cm sec<sup>-1</sup>, typical seasonal ranges may be up to an order of magnitude larger. The results are rather smooth representations in which much of the temporal and spatial detail available in finer scale summaries (Wyllie, 1966; Hart and Currie, 1960; Robles, 1979) has been filtered out. No attempt has been made to extrapolate the dynamic height calculations into shallow coastal regions (i.e., bottom depths less than 1000 m). Where these summaries do not depict major circulation features near the coast, the predominant flow directions have been indicated by shaded arrows (e.g., over the Agulhas Bank and in the Southern California Bight).

Characteristic vertical sections of oxygen (Figs. 3,4) and density (Figs. 5,6) along predominantly meridional axes of the eastern boundary current systems were also constructed from the large-scale analyses. The locations of the sections are shown in Figure 1. Although the sections lie up to several hundred kilometers from the coast, the general features (e.g., oxygen minima) are felt to be representative of the coastal regimes, as well. Values of oxygen (mL L<sup>-1</sup>) defined at standard depths between the surface and 1500 m are contoured with an interval of 0.5 mL L<sup>-1</sup>. Oxygen minima (values less than 1.0 mL L<sup>-1</sup>) are indicated by cross-hatching. Analogous sections of density (sigma-t) were derived from the annual mean values of temperature and salinity in the upper 500 m of the water column. Values of sigma-t are contoured with an interval of 0.2. On each vertical section, the latitudinal locations associated with prominent coastal features (e.g., capes and coastal cities) are designated by simple letter abbreviations. The reader is directed to Figure 1 and to Chart 1 for proper orientation of each section.

Historical mechanical bathythermograph (MBT) profiles and hydrocast data (temperature and salinity versus depth) archived in the Master Oceanographic Observation Data Set (MOODS) at the U.S. Navy's Fleet Numerical Oceanography Center (FNOC) in Monterey, California were used to calculate indices of mixed layer depth (Table 5) and selected profiles of vertical stability (Fig. 8). Mixed layer depths (in meters) were defined and calculated as described by Husby and Nelson (1982). The vertical gradient of sigma-t was used as an index of the static stability (E) of the water column, as suggested by Hesselberg and Sverdrup (1915; cited in Sverdrup, Johnson, and Fleming, 1942). Bimonthly vertical profiles of static stability ( $E \times 10^6 \text{ m}^{-1}$ ) in the upper 300 m are displayed for three locations in the Benguela Current system (Fig. 8).

---

## SURFACE MARINE DATA

The climatological distributions of sea surface temperature, coastal-oceanic temperature contrast, surface layer Ekman transport, wind-generated turbulent energy production, and total cloud amount presented in this appendix are based on summaries of data contained in the National Climatic Center's (NCC) file of surface marine observations (Tape Data Family-11). The total file contains in excess of 50 million individual ship reports dating from the mid-19th century through 1979. Over 3.3 million of the reports are from the area of the Canary Current system. Summaries for the California and Benguela Current regions are based on 1.9 million and 1 million individual reports, respectively. The area off western South America contains an order of magnitude fewer surface weather observations (0.3 million).

Long-term composite summer and winter distributions of surface atmospheric properties were compiled by 1-degree latitude and longitude quadrangles within the four geographical regions outlined in Figure 1. The boundaries of the summary grids are defined as follows:

1. California Current - extends from lat.  $20^{\circ}$  N to  $50^{\circ}$  N and from the coast to 15 degrees of longitude offshore.
2. Peru Current - extends from lat.  $50^{\circ}$  S to  $4^{\circ}$  S and from the coast to 14 degrees of longitude offshore.
3. Canary Current - extends from lat.  $5^{\circ}$  N to  $45^{\circ}$  N and from the coast to 15 degrees of longitude offshore.
4. Benguela Current - extends from lat.  $39^{\circ}$  S to  $8^{\circ}$  S and from long.  $35^{\circ}$  E to  $2^{\circ}$  E; off the southwest coast, the data extend from the coast to 11 degrees of longitude offshore.

In each case, the data grid parallels the coastline configuration and each 1-degree quadrilateral is centered on a whole degree of latitude and longitude. All observations available in the TDF-11 file within the summary regions were averaged over six, two-month periods. Therefore, a mean value for each two-month period and square is formed from a data set which is independent of all other months and squares. Although all six bimonthly distributions were examined, we selected the January-February and July-August fields to represent the characteristic distributions for summer and winter seasons in the respective hemispheres.

The observations contained in the TDF-11 file vary markedly in methods and precision of measurement due to the changes in instrumentation, sampling techniques, and reporting procedures over the considerable time period covered by the data base. Based on the documentation for the TDF-11 data file<sup>4/</sup>, a single pass editor was used to remove gross errors in the data, including erroneous position reports, and observations of sea surface temperature, wind speed and direction, and cloud amount exceeding extreme value limits. Detailed discussions of the sources of measurement errors and techniques for more refined data editing may be found in Bakun, McLain, and Mayo (1974), Nelson (1977), and Nelson and Husby (1983).

The spatial distributions of surface marine observations are known to be biased to the coastwise and transoceanic shipping lanes between major seaports. Chart 2 shows the distribution of total numbers of observations per 1-degree quadrangle in each boundary current region. A contour interval of 5,000 has been used and values exceeding 10,000 observations per 1-degree square are shaded. However, note that for the Peru Current region, the contour interval is 500 and values greater than 1000 observations per 1-degree square are shaded. In most cases, the highest density of reports lies within 300 km of the coast, except off southwestern Africa, where the narrow main shipping lane diverges sharply from the coast north of Cape Columbine. The numbers of reports per 1-degree square range from fewer than 50 off Peru and Chile to more than 40,000 in the Southern California Bight and off the Iberian Peninsula. Summer and winter averages are most reliable within the well traveled shipping lanes, but less precise in the offshore regions. Some temporal bias may also exist, since approximately 60-80 percent of the total reports have been taken since 1950.

<sup>4/</sup> National Climatic Center, Tape Data Family 11, NOAA/EDIS/NCC, Asheville, N.C.

---

The composite distributions are based on independent 1-degree square sample means. Detail within a single square which is not supported by similar values in surrounding squares reflects sampling error. Therefore, when contoured fields have been used to display the results of this study, the mean distributions have been machine contoured, subjectively smoothed, and recontoured to remove extreme values which were not supported by data in directly adjacent squares. Typically, "bull's-eyes" in the contoured fields reflected a paucity of ship observations or inadequate sampling of extreme events.

#### Sea Surface Temperature- Charts 3 and 4

Summer and winter distributions of sea surface temperature ( $^{\circ}\text{C}$ ) are contoured at intervals of  $1^{\circ}\text{C}$ . Seasonal cycles of sea surface temperature at selected coastal locations in each boundary current are listed in Table 4.

#### Coastal Temperature Anomaly - Charts 5 and 6

Summer and winter distributions of coastal temperature anomaly were constructed from the corresponding fields of sea surface temperature as follows. A smoothed offshore temperature reference was constructed by successively applying, at each 1-degree latitude increment, a 5-degree latitude by 3-degree longitude moving-average filter centered at the tenth 1-degree square from the coast. Sampling irregularities were reduced by discarding the three highest and three lowest values of the fifteen sample averages covered by the filter at each step, and averaging the remaining nine values. The value of this offshore reference temperature at the proper latitude was subtracted from each 1-degree averaged sea surface temperature. The coastal temperature anomaly, therefore, is the difference between the sea surface temperature at each location and the large-scale temperature offshore. The method is similar to that used by Böhnecke (1936; cited in Wooster and Reid, 1963) to describe the Canary Current and Benguela Current upwelling systems, in that it attempts to filter the basin-wide meridional temperature gradient, thereby highlighting local effects.

Temperature anomalies ( $^{\circ}\text{C}$ ) are contoured with an interval of  $1^{\circ}\text{C}$ . Anomalies less than  $-2^{\circ}\text{C}$  are shaded. Cross-hatching designates positive anomalies greater than  $1^{\circ}\text{C}$ . Negative anomalies indicate that the mean sea surface temperature is colder than the offshore reference temperature; positive values indicate the opposite.

#### Ekman Transport - Charts 7 and 8

Surface wind reports from the TDF-II data file were used to construct summer and winter distributions of surface layer Ekman transport in each of the eastern boundary current regions. Ekman transport is calculated as the ratio of the wind stress magnitude to the local value of the Coriolis parameter, and is directed  $90^{\circ}$  to the right (left) of the surface wind stress in the northern (southern) hemisphere. The method of calculation is described by Bakun et al. (1974). To clarify the presentations, vector symbols are only plotted for alternate 1-degree squares in both latitude and longitude coordinates. Ekman transport is plotted in units of metric tons per second per meter ( $\text{t sec}^{-1} \text{m}^{-1}$ ), and vector symbols are scaled according to the key on the charts.

Scatter diagrams of Ekman transport versus the cube of the wind speed (Fig. 7) are used to distinguish between regimes characterized by strong surface layer transport and those dominated by wind-generated turbulence. At selected locations along each coast, vector means were resolved into components perpendicular and parallel to the coast. Coastline angles were determined by visually fitting a line to the dominant trend of the coast. Estimates of the offshore (onshore) directed component of Ekman transport are plotted against the cube of the wind speed in Figure 7.

---

Wind Speed Cubed - Charts 9 and 10

The rate at which turbulent kinetic energy of the wind is added to the upper ocean and becomes available to mix the stable thermocline layers is proportional to the third power, or "cube" of the wind speed (Niiler and Kraus, 1977). Mean summer and winter distributions of the cube of the surface wind speed were compiled from the TDF-11 surface wind reports following the methods of Husby and Nelson (1982). Mean values are plotted in units of  $1000 \text{ m}^3 \text{ sec}^{-3}$  and contoured with an interval of  $250 \text{ m}^3 \text{ sec}^{-3}$ . One-degree means of wind speed cubed at selected locations in each boundary current are plotted against offshore (onshore) Ekman transport in Figure 7.

Total Cloud Amount - Charts 11 and 12

Mean distributions of total cloud amount were assembled from the TDF-11 data file following procedures modified from Nelson and Husby (1983). Mean values are plotted in units of tenths of sky obscured and the contour interval is one-tenth. Based on the general patterns of cloud cover, certain inferences may be made about the expected distributions of net insolation. In particular, it should be noted that the summer distributions (Chart 11) show relative cloud cover minima at coastal locations characterized as centers of upwelling (e.g., Cape Mendocino, Cap Blanc to Cabo Bojador, Talcahuano, and Cape Columbine to Lüderitz). One implication of these distributions is that higher levels of incoming shortwave radiation reach the sea surface in the highly productive upwelling regions than elsewhere in the eastern boundary current systems (Bakun and Nelson, 1977; Nelson and Husby, 1983).

---

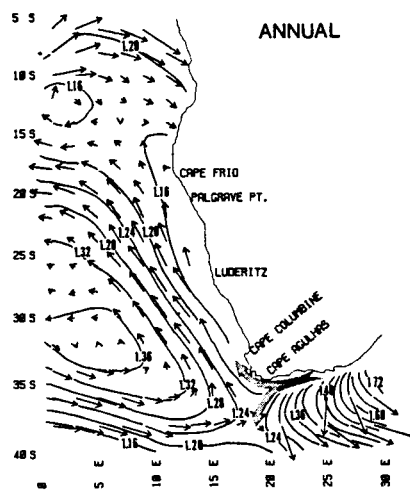
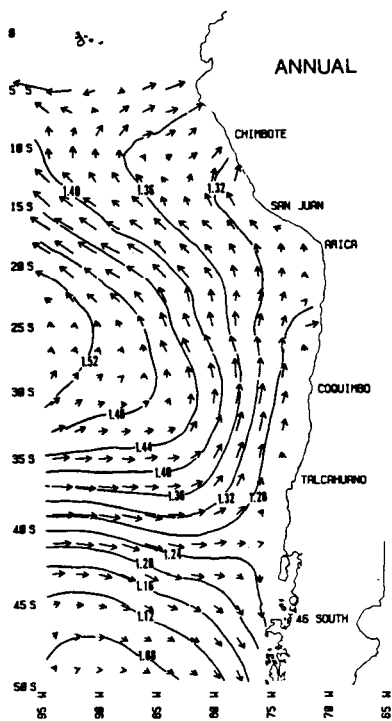
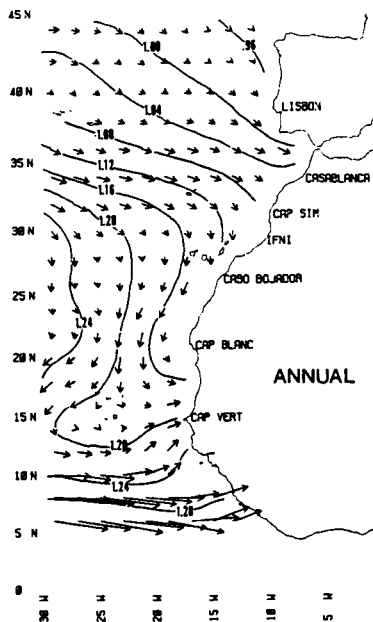
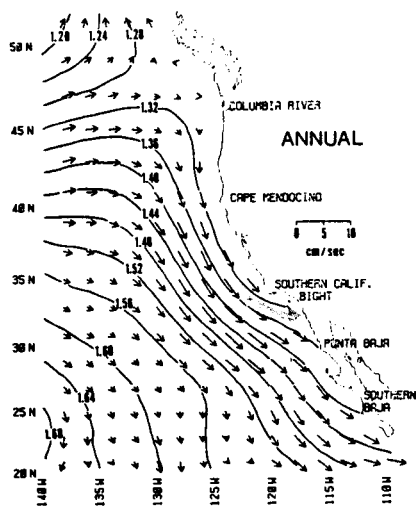


Chart 1. Annual mean surface geostrophic flow (0/1000 db,  $\text{cm sec}^{-1}$ ) and dynamic topography (dyn m).



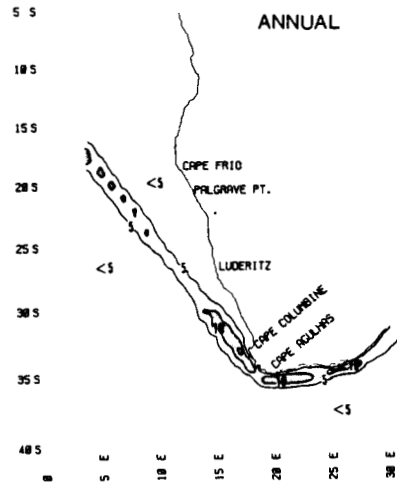
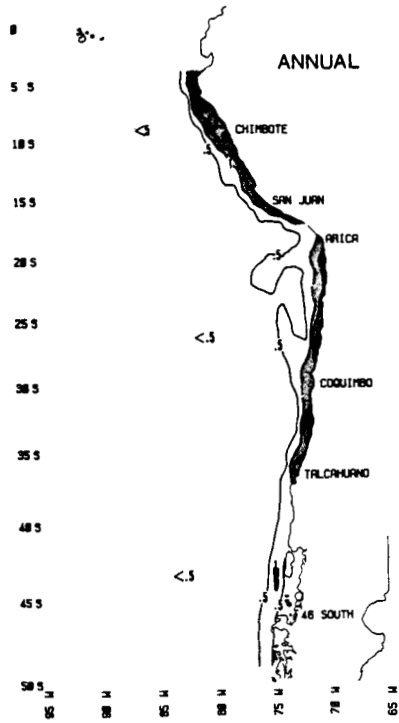
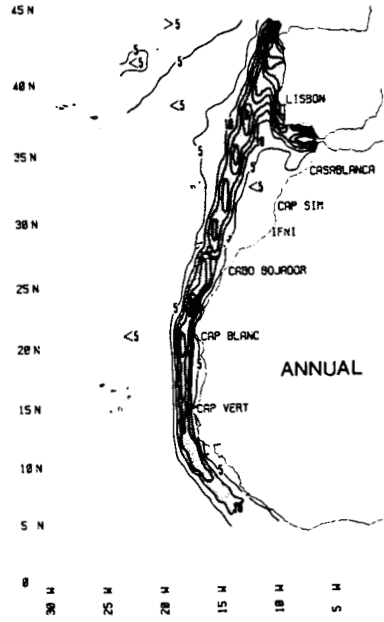
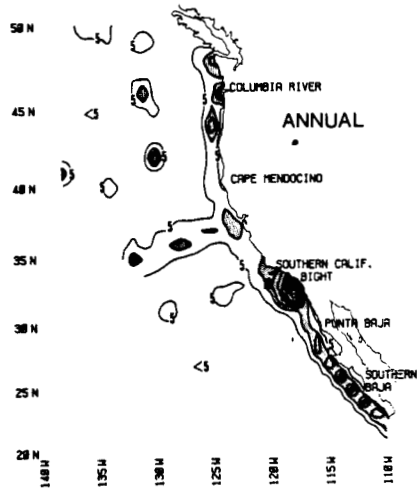


Chart 2. Distributions of observations per 1-degree square (thousands of observations)

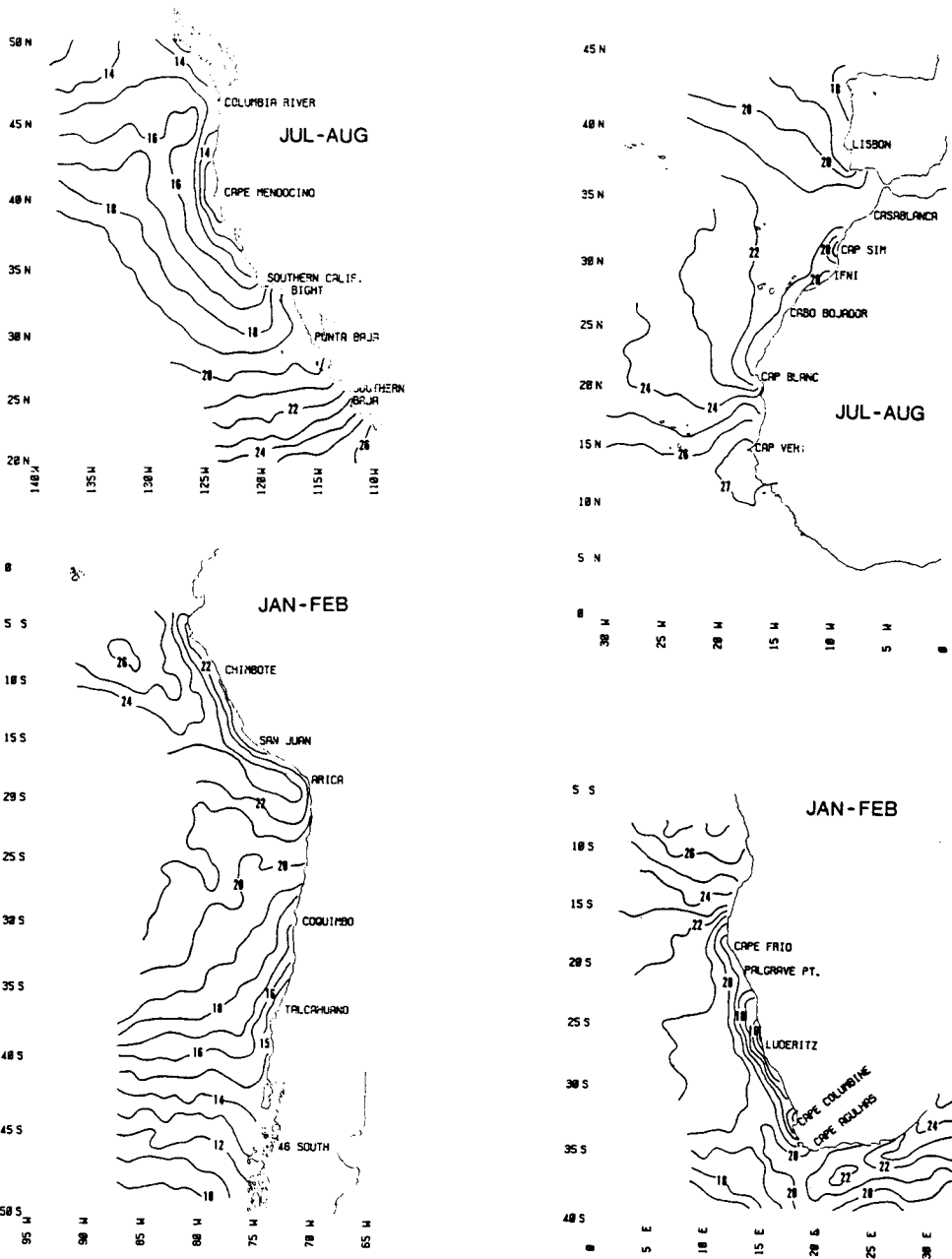


Chart 3. Summer sea surface temperature ( $^{\circ}$ C).

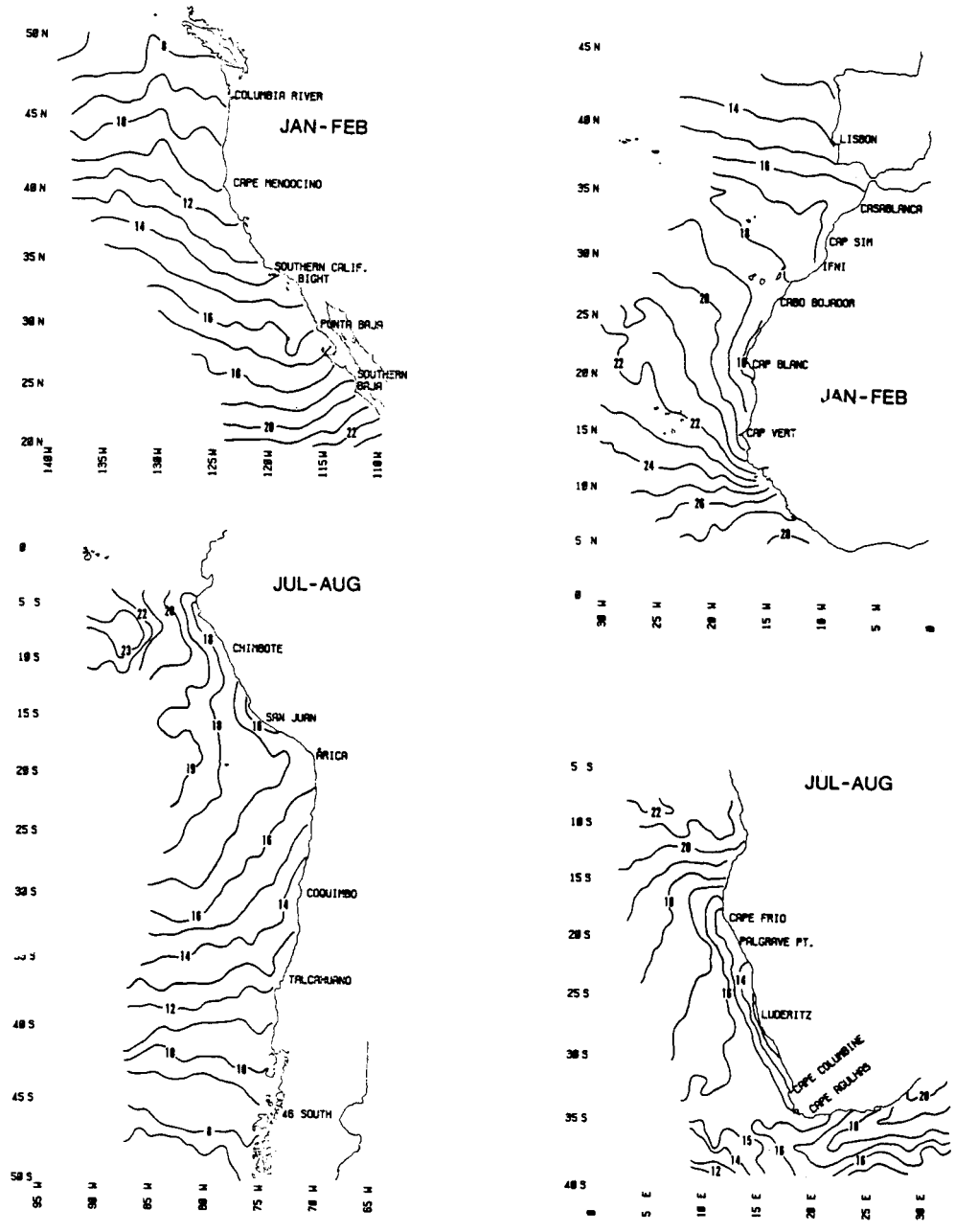


Chart 4. Winter sea surface temperature ( $^{\circ}$ C).

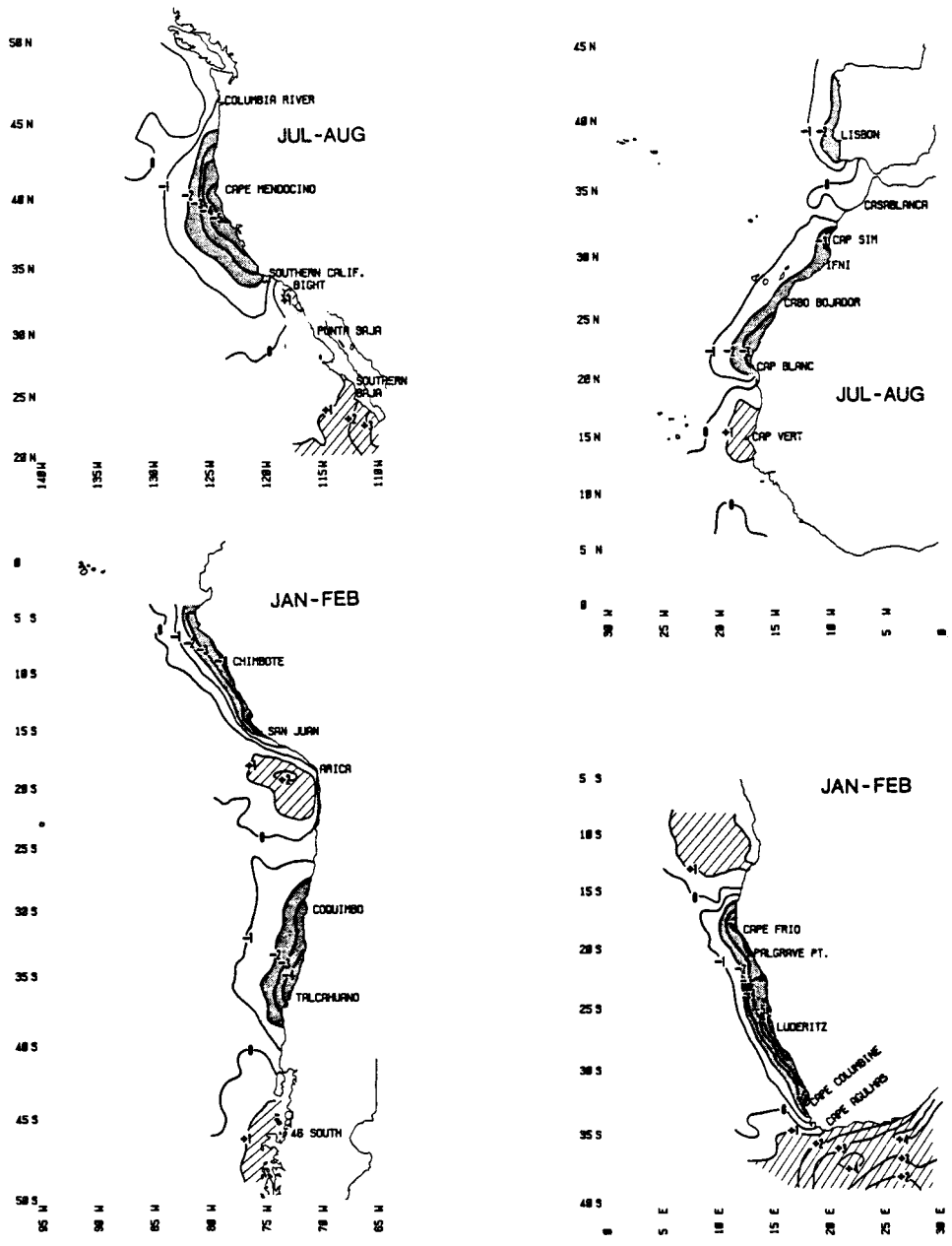


Chart 5. Summer coastal sea surface temperature anomaly ( $^{\circ}$ C).

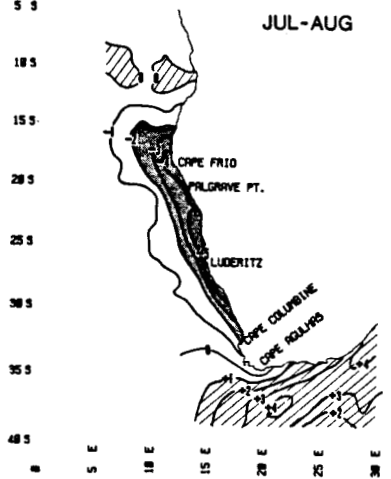
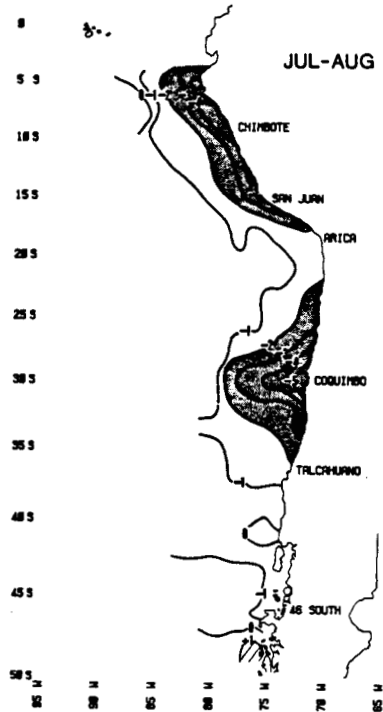
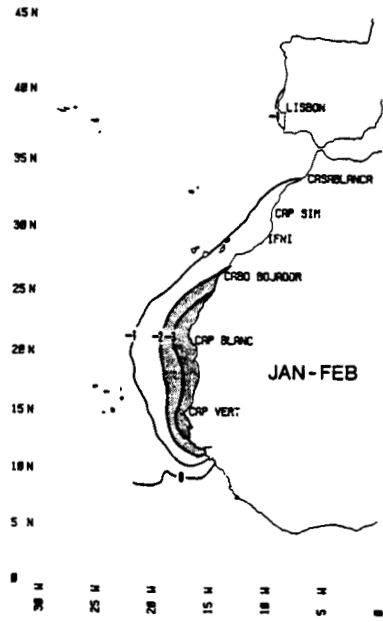
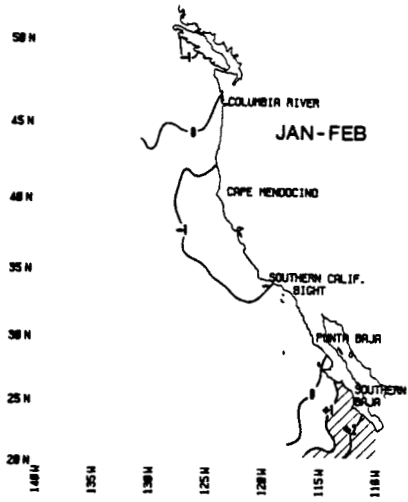


Chart 6. Winter coastal sea surface temperature anomaly ( $^{\circ}$ C).

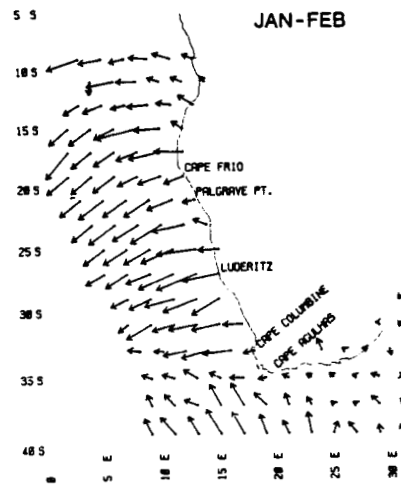
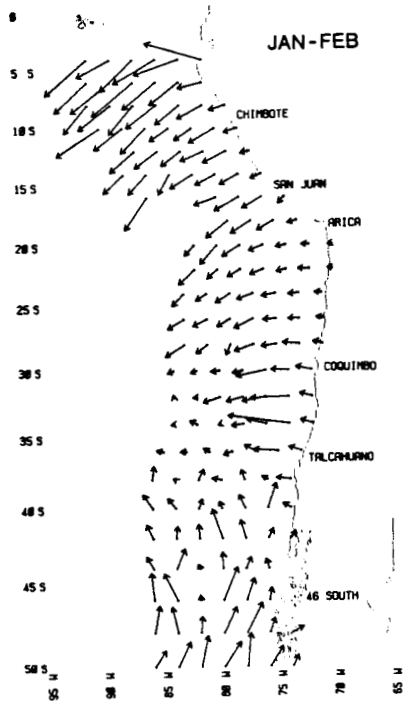
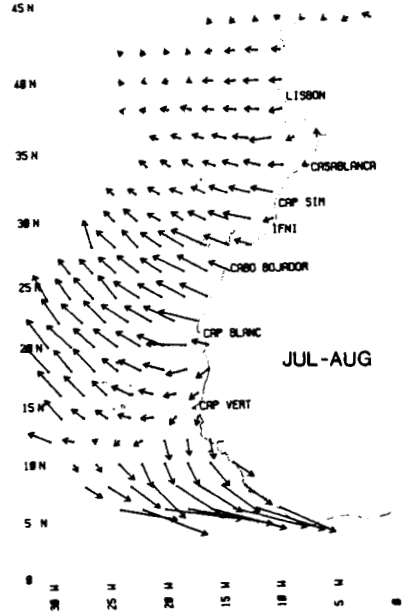
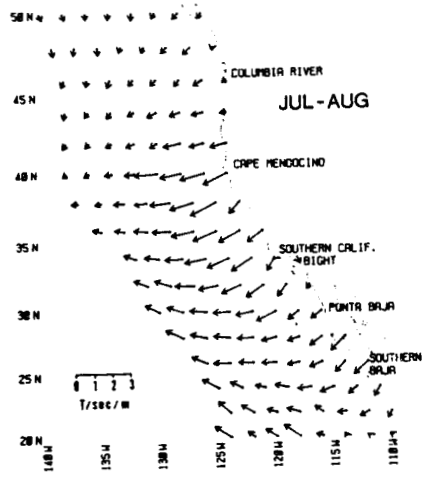


Chart 7. Summer surface Ekman transport ( $t \text{ sec}^{-1} \text{ m}^{-1}$ )

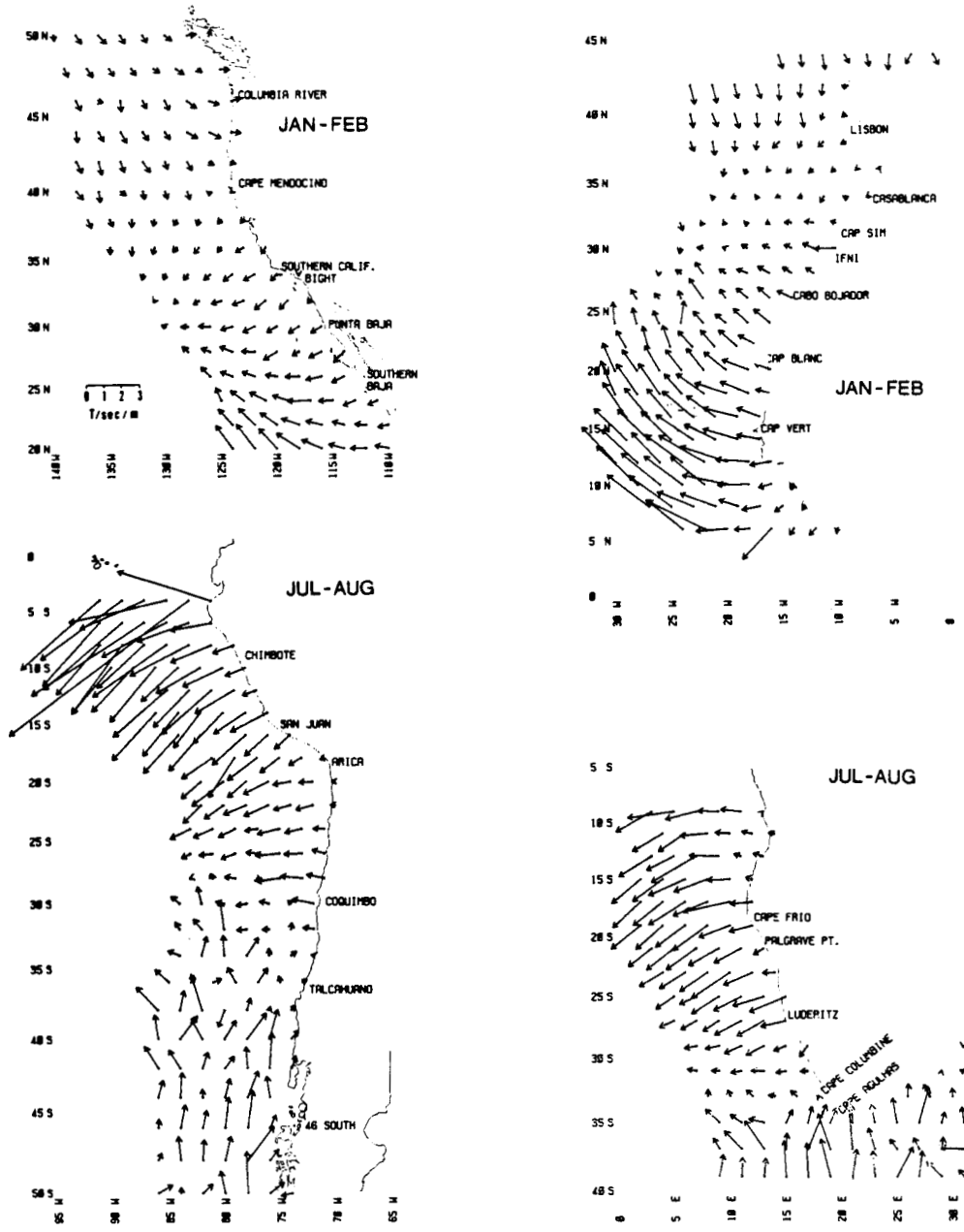


Chart 8. Winter surface Ekman transport ( $t \text{ sec}^{-1} \text{ m}^{-1}$ )

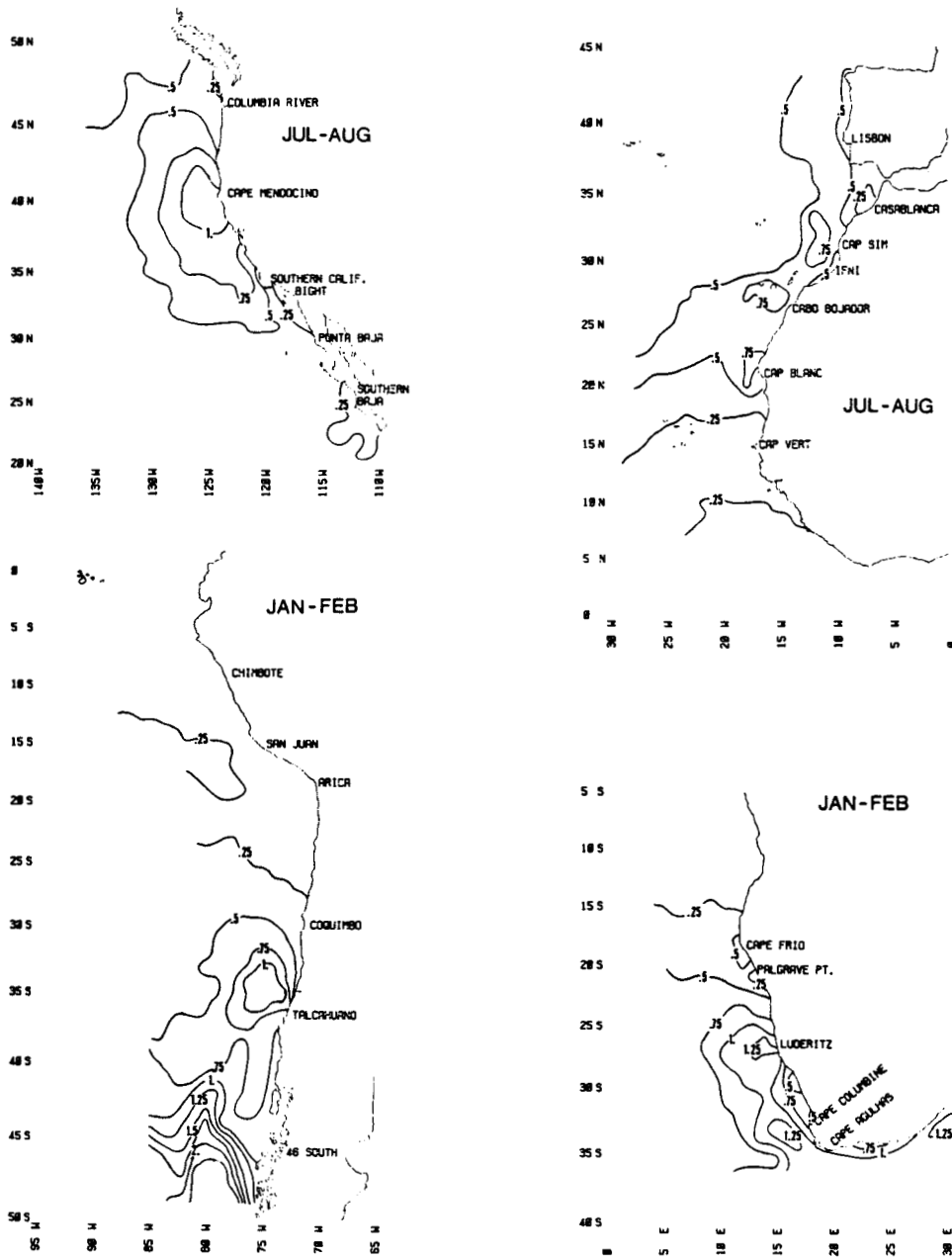


Chart 9. Summer distributions of wind speed cubed (units of  $1000 \text{ m}^3 \text{ sec}^{-3}$ ).



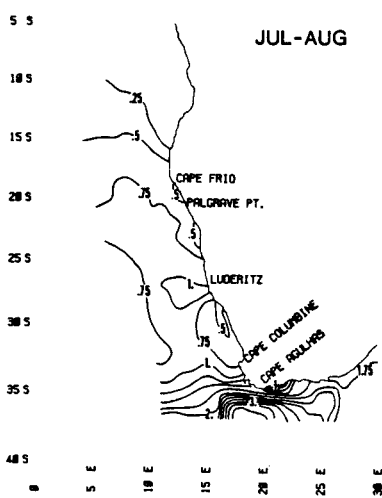
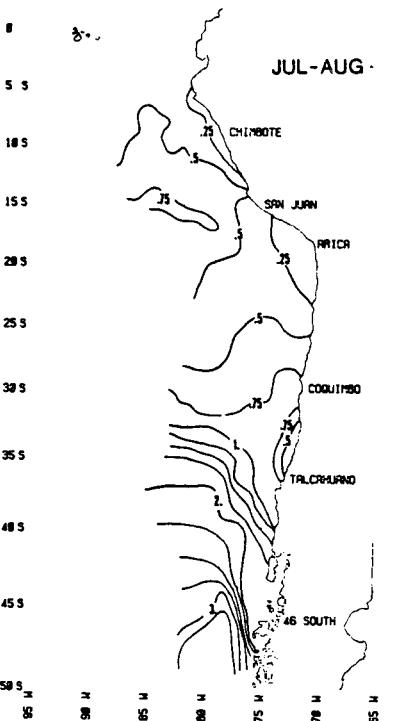
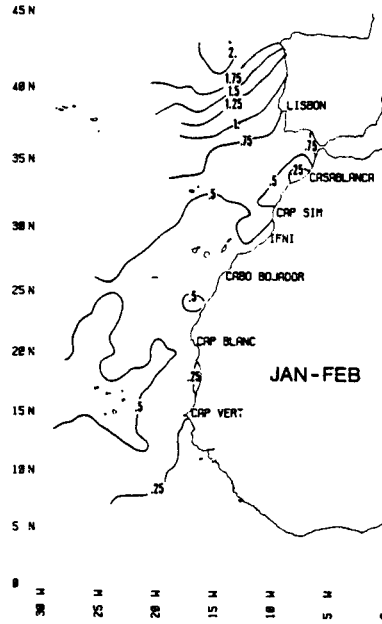
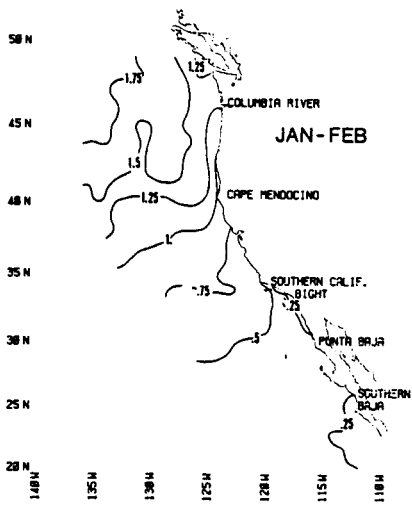


Chart 10. Winter distributions of wind speed cubed (units of  $1000 \text{ m}^3 \text{ sec}^{-3}$ ).

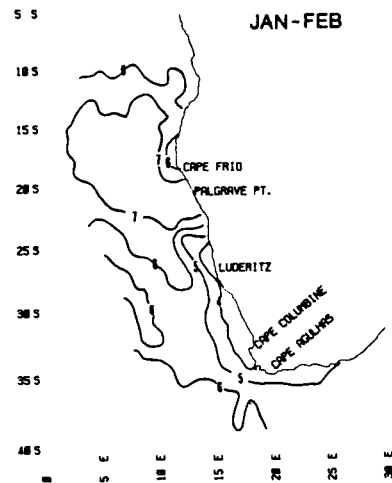
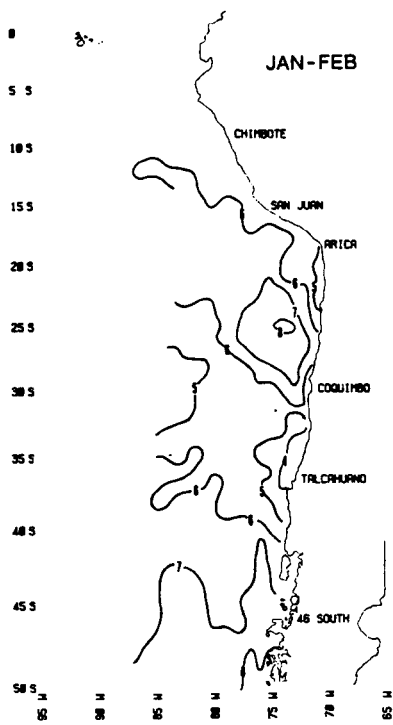
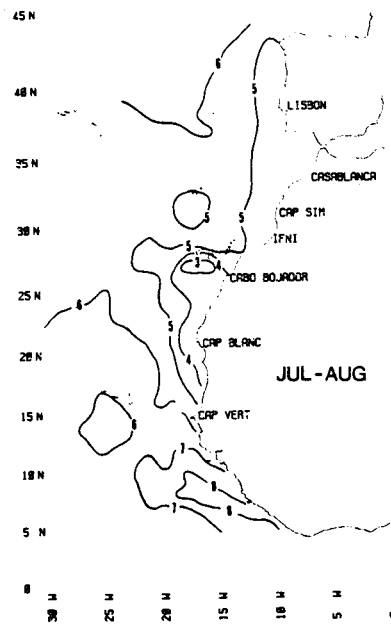
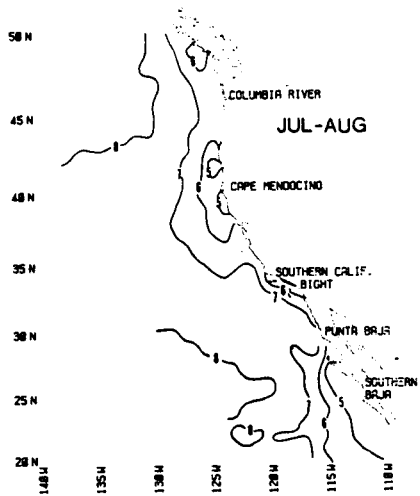


Chart 11. Summer distributions of total cloud amount (tenths of sky obscured).

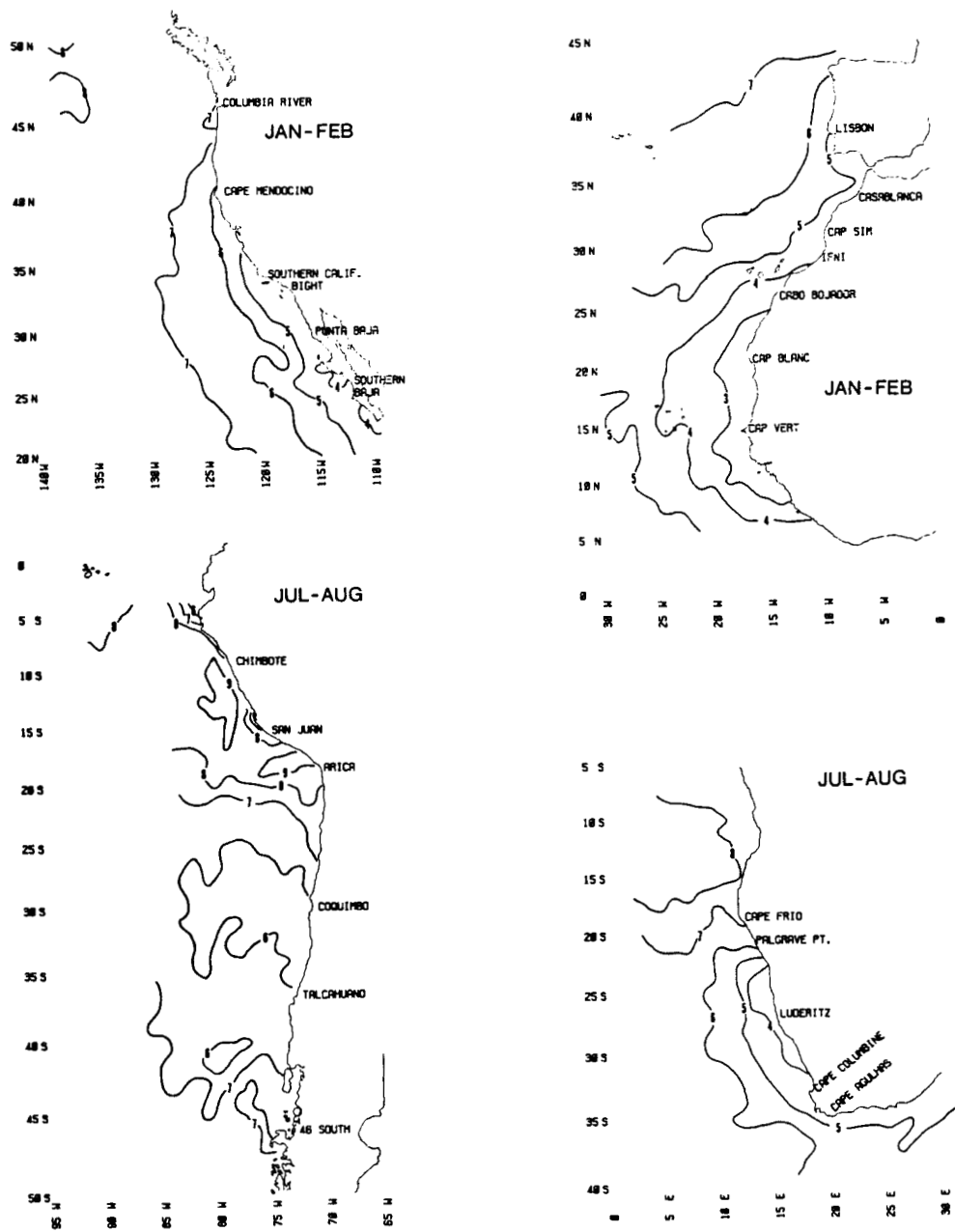


Chart 12. Winter distributions of total cloud amount (tenths of sky obscured).

REFERENCES

- Ahlstrom, E.H. 1959. Vertical distribution of pelagic fish eggs and larvae off California and Baja California. U.S. Fish Wildl.Serv., Fish.Bull. 60:107-146.
- \_\_\_\_\_. 1965. Kinds and abundance of fishes in the California Current region based on egg and larval surveys. Calif.Coop.Oceanic Fish.Invest., Rep. 10:31-52.
- Badenhorst, A. and A.J. Boyd. 1980. Distributional ecology of the larvae and juveniles of the anchovy Engraulis capensis Gilchrist in relation to the hydrological environment off South West Africa, 1978/79. Fish.Bull.S.Afr. 13:83-106.
- Bakun, A. 1973. Coastal upwelling indices, west coast of North America, 1946-71. U.S. Dep.Commer. NOAA Tech.Rep.NMFS SSRF-671, 103 p.
- Bakun, A. and C.S. Nelson. 1977. Climatology of upwelling related processes off Baja California. Calif. Coop.Oceanic Fish.Invest.Rep. 19:107-127.
- Bakun, A. and R.H. Parrish. 1980. Environmental inputs to fishery population models for eastern boundary current regions. In Workshop on the effects of environmental variation on the survival of larval pelagic fishes, Lima, Peru. 20 April-5 May 1980. IOC Workshop Rep. 28, UNESCO, Paris, p. 67-104.
- \_\_\_\_\_. 1982. Turbulence, transport and pelagic fish in the California and Peru Current systems. Calif.Coop.Oceanic Fish.Invest.Rep. 23:99-112.
- Bakun, A., D.R. McLain and F.V. Mayo. 1974. The mean annual cycle of coastal upwelling off western North America as observed from surface measurements. Fish.Bull., U.S. 72(3):843-844.
- Bang, N.D. and W.R.H. Andrews. 1974. Direct current measurements of a shelf-edge frontal jet in the southern Benguela system. J.Mar.Res. 32(3):405-417.
- Barkley, R.A. 1968. Oceanographic Atlas of the Pacific Ocean. Univ. of Hawaii Press, Honolulu, 20 p., 156 charts.
- Belveze, H. and J. Bravo de Laguna. 1980. Les ressources halieutiques de l'atlantique centre-est. Deuxieme partie: Les ressources de la cote ouest-africaine entre 24°N et le Detroit de Gibraltar. FAO Doc.Tech.sur les peches, FIRM/T 186.2 (Fr.) 64 p.
- Bernstein, R.L., L. Breaker and R. Whritner. 1977. California Current eddy formation: ship, air and satellite results. Science. 195:353-359.
- Bohnecke, G. 1936. Temperatur, Salzgehalt und Dichte an der Oberflache des Atlantischen Ozeans. Atlas. "Meteor" Rep. 5. 74 charts.
- Bravo de Laguna, J., M.A.R. Fernandez and J.C. Santana. 1976. The Spanish fishery on sardine (Sardina pilchardus Walb.) off West Africa. ICES CM 1977/G:13 Pelagic Fish (Southern) Committee.
- Cañon, J.R. 1978. Distribución de la anchoveta (Engraulis ringens Jenyns) en el norte de Chile en relación a determinadas condiciones oceanográficas. Invest.Pesq.Inst.Fom.Pesq. Santiago, Chile. 30, 128 p. (Also available in English: J.R. Cañon, Distribution of anchoveta (Engraulis ringens Jenyns) in northern Chile in relation to selected oceanographic conditions, M.S. thesis, Oregon State University, Corvallis, 1973. 106 p.
- Cram, D. 1981. Hidden elements in the development and implementation of marine resource conservation policy: The case of the South West Africa/Namibian fisheries. In Resource management and environmental uncertainty. (M.H. Glantz and J.D. Thompson, eds). John Wiley and Sons, New York. p. 137-158.
- Crawford, R.J.M. 1980. Seasonal patterns in South Africa's western cape purse-seine fishery. J.Fish.Biol. 16:649-664.
-

- Crawford, R.J.M., P.A. Shelton and L. Hutchings. 1980. Implications of availability, distribution and movements of pilchard sardinops ocellata and anchovy Engraulis capensis for assessment and management of the South African purse-seine fishery. Rapp.P.-v.Reun.Cons.int.Explor.Mer. 177:355-373.
- Darbyshire, M. 1966. The surface waters near the coasts of southern Africa. Deep-Sea Res. 13(1):57-81.
- Ekman, V.W. 1905. On the influence of the earth's rotation on ocean currents. Ark.Mat.Astron.Fys. 2(11):1-55.
- Food and Agriculture Organization of the United Nations. 1978. Report of the ad hoc working group on sardine (Sardina pilchardus Walb.) CECAF/ECAF Series/78/7(En), 35 p.
- Guillen, O. 1980. The Peru current system. I: Physical aspects. In Proceedings of the workshop on the phenomenon known as "El Niño". UNESCO, Paris:185-216. In English and Spanish.
- Gunther, G.R. 1936. A report on oceanographical investigations in the Peru Coastal Current. Discovery Rep. 13:17-276.
- Hart, T.J. and R.I. Currie. 1960. The Benguela Current. Discovery Rep., 31:123-298.
- Hessleberg, T.H. and H.U. Sverdrup. 1915. Die Stabilitätsverhältnisse des Seewassers bei vertikalen Verschiebungen. Bergens Museums Aarbok 1914-15. No. 15, 16 p.
- Hickey, B.M. 1979. The California Current System - hypotheses and facts. Progress in Oceanography, 8(4):191-279.
- Husby, D.M. and C.S. Nelson. 1982. Turbulence and vertical stability in the California Current. Calif.Coop.Oceanic Fish.Invest.Rep. 23:113-129.
- Hughes, P. and E.D. Barton. 1974. Stratification and water mass structure in the upwelling area off northwest Africa in April/May 1969. Deep-Sea Res., 21:611-628.
- Huyer, A. 1976. A comparison of upwelling events in two locations: Oregon and Northwest Africa.J.Mar.Res. 34(4):531-546.
- Jordán, R.S. 1980. Biology of the anchoveta: I. Summary of the present knowledge. In Proceedings of the workshop on the phenomenon known as "El Niño". UNESCO, Paris: 249-278. In English and Spanish.
- King, D.P.F. 1977. Distribution and relative abundance of eggs of South West African pilchard Sardinops ocellata and anchovy Engraulis capensis, 1971/72. Fish.Bull.S.Afr., 9:23-31.
- Kramer, D. and J.R. Zweifel. 1970. Growth of anchovy larvae (Engraulis mordax Girard) in the laboratory as influenced by temperature. Calif.Coop.Oceanic Fish.Invest.Rep. 14:84-87.
- Lafond, E.C. 1951. Processing oceanographic data. U.S. Navy Hydrographic Office, H.O.Pub. No. 614, Washington, D.C. 114 pp.
- Lasker, R. 1964. An experimental study of the effects of temperature on the incubation time, development and growth of Pacific sardine embryos and larvae. Copeia, No. 2:399-405.
- \_\_\_\_\_. 1978. The relation between oceanographic conditions and larval anchovy food in the California Current: identification of factors leading to recruitment failure. Rapp.P.-v.Reun.Cons.int.Explor.Mer. 173:212-230.
- Le Clus, F. 1979. Oocyte development and spawning frequency in the South West African pilchard Sardinops ocellata. Fish.Bull.S.Afr. 12:53-68
- Levitus, S. 1982. Climatological Atlas of the World Ocean. U.S.Dep.Commer., NOAA Prof.Pap. 13. 173 p.
-

- Levitus, S. and A.H. Oort. 1977. Global analysis of oceanographic data. *Bull.Amer.Meteor.Soc.* 58(12):1270-1284.
- McDowell, S.B. 1962. Personal letter to A.J. Liebling. p. 189-202. In A.J. Liebling, "Onward and upward with the arts: The soul of bouillabaisse". *The New Yorker*, October 27, 1962.
- Mittelstaedt, E. 1974. Some aspects of the circulation in the north-west African upwelling area off Cap Blanc. *Tethys*, 6(1-2):89-92.
- Moers, C.N.K. and J.S. Allen. 1973. Final report of the Coastal Upwelling Ecosystems Analysis Summer 1973. Theoretical Workshop. School of Oceanography, Oregon State Univ. Corvallis, Oregon. 212 p.
- Nelson, C.C. 1977. Wind stress and wind stress curl over the California Current. U.S. Dep.Commer. NOAA Tech.Rep. NMFS SSRF-714, 87 p.
- Nelson, C.S. and D.M. Husby. 1983. Climatology of surface heat fluxes over the California Current region. U.S.Dep.Commer. NOAA Tech.Rep. NMFS SSRF-763, 155 p.
- Nelson, G. and L. Hutchings. MS. The Benguela upwelling area. Sea Fisheries Institute, Cape Town, South Africa, 32 p.
- Neumann, G. and W.J. Pierson, Jr. 1966. Principles of Physical Oceanography, Prentice-Hall, Englewood Cliffs, 545 p.
- Niller, P.P. and E.B. Kraus. 1977. One-dimensional models of the upper ocean. p. 143-172. In Modelling and prediction of the upper layers of the ocean. (E.B. Kraus, ed.) Pergamon Press, New York,
- Parrish, R.H., C.S. Nelson and A. Bakun. 1981. Transport mechanisms and reproductive success of fishes in the California Current. *Biol. Oceanogr.* 1(2):175-203.
- Pauly, D. 1981. The relationships between gill surface area and growth performance in fish: a generalization of von Bertalanffy's theory of growth. *Meeresforschung.* 28:251-282.
- Pavlova, Y.V. 1966. Seasonal variations of the California Current. *Oceanol.* 6(6):806-814.
- Radovich, J. 1981. The collapse of the California sardine fishery: what have we learned? p. 107-306. In Resource management and environmental uncertainty: lessons from coastal upwelling fisheries. (M.H. Glantz and J.D. Thopson, eds.) John Wiley and Sons, New York.
- Rebert, J.P. 1978. Note on the hydrology of the west African continental shelf, from Mauritania to Guinea (Annex 9). p. 87-92. In Report of the ad hoc working group on West African coastal pelagic fish from Mauritania to Liberia (26°N to 5°N). CEEAF/ECAF Series 78/10 (En).
- Reed, R.K. and D. Halpern. 1976. Observations of the California Undercurrent off Washington and Vancouver Island. *Limnol.Oceanogr.* 21(3):389-398.
- Reid, J.L., Jr. 1967. Oceanic environments of the genus Engraulis around the world. *Calif.Coop.Oceanic Fish.Invest.* Rep. 11:29-33.
- Reid, J.L., Jr., G.I. Roden and J.G. Wyllie. 1958. Studies of the California Current System. *Calif.Coop.Oceanic Fish.Invest., Prog.Rep.*, 1 July 1956 to 1 January 1958. p. 27-57.
- Robles, F.L.E. 1979. Water masses and circulation in the S.E. Pacific and the "El Nino" event. Ph.D. Thesis, University of Wales, Swansea, 175 p. 156 charts.
- Santander, H. and O.S. de Castillo. 1979. El ictioplancton de la Costa Peruana. *Bol.Inst.Mar.Peru.* 4(3):69-112.
- Serra, J.B., M.H. Aguayo, O.J. Rojas, F.C. Inostroza and J.C. Canon. 1979. Sardina Española. 37 p. In Estado actual de principales pesquerias nacionales. Instituto de Fomento Pesquero, Chile,
-

- Shannon, L.V. 1970. Oceanic circulation off South Africa. *Fish.Bull.S.Afr.* 6:27-33.
- Shelton, P.A. and L. Hutchings. 1982. Transport of anchovy, *Engraulis capensis* Gilchrist, eggs and early larvae by a frontal jet current. *J.Cons.int.Explor.Mer.* 40:185-198.
- Silva, S.N. and S. Neshyba. 1979. On the southernmost extension of the Peru-Chile Undercurrent. *Deep-Sea Res.* 26A:1387-1393.
- Smith, R.L. 1978. Physical oceanography of coastal upwelling regions. A comparison: Northwest Africa, Oregon and Peru. Symposium on the Canary Current: Upwelling and Living Resources, No. 40, 10 p.
- Stander, G.H. 1964. The pilchard of South West Africa. The Benguela Current off South West Africa. *Investl.Rep.Mar.Res.Lab., S.W.Afr.* 12, 122 p.
- Stander, G.H. and A.H.B. de Decker. 1969. Some physical and biological aspects of an oceanographic anomaly off South West Africa in 1963. *Investl.Rep.Div.Sea Fish.S.Afr.* 81:1-46.
- Sverdrup, H.U. and R.H. Fleming. 1941. The waters off the coast of Southern California, March to July 1937. *Bull.Scripps Inst.Oceanogr. Univ. of Calif. La Jolla.* 4:261-378.
- Sverdrup, H.U., M.W. Johnson and R.H. Fleming. 1942. The oceans: their physics, chemistry and general biology. Prentice-Hall, Englewood Cliffs. 1087 p.
- Tomczak, M., jr. 1981. Prediction of environmental changes and the struggle of the third world for national independence: The case of the Peruvian fisheries. p. 401-438. *In* Resource management and environmental uncertainty. (M.H. Glantz and J.D. Thompson, eds.) John Wiley and Sons, New York.
- Troadee, J.-P., W.G. Clark and J.A. Gulland. 1980. A review of some pelagic fish stocks in other areas. *Rapp.P.-v.Reun.Cons.int.Explor.Mer.* 177:252-277.
- Wooster, W.S. and J.H. Jones. 1970. California undercurrent off northern Baja California. *J.Mar.Res.* 28(2):235-250.
- Wooster, W.S. and J.L. Reid, Jr. 1963. Eastern boundary currents. p. 253-280. *In* The Sea. Vol. 2. (M.N. Hill, ed.) Interscience Publ., New York.
- Wooster, W.S. and H.A. Sievers. 1970. Seasonal variations of temperature, drift, and heat exchange in surface waters off the west coast of South America. *Limnol.Oceanogr.* 15:595-605.
- Wylie, J.G. 1966. Geostrophic flow of the California Current at the surface and at 200 m. *Calif.Coop.Oceanic Fish.Invest., Atlas No. 4, XXII* p, 288 charts.
- Wyrtki, K. 1965. Summary of the physical oceanography of the eastern Pacific Ocean. *Inst. of Mar.Res.Ref.* 65-10, Scripps Inst.Oceanogr., Univ. of Calif., La Jolla. 69 p. 9 charts.
-